NASA-CR-195242

A semi-annual report for

STUDIES OF EXTRA-SOLAR OORT CLOUDS AND THE KUIPER DISK

NASA Grant No.: NAGW-3023

SwRI Project No.: 15-4971

Submitted by:

Dr. S. Alan Stern, Principal Investigator
Space Sciences Division
Southwest Research Institute
San Antonio, Texas

March 22, 1994

SOUTHWEST RESEARCH INSTITUTE
Instrumentation and Space Research Division
6220 Culebra Road, San Antonio, Texas 78238
(512) 684-5111 • FAX (512) 647-4325

A semi-annual report for

STUDIES OF EXTRA-SOLAR OORT CLOUDS AND THE KUIPER DISK

NASA Grant No.: NAGW-3023

SwRI Project No.: 15-4971

Submitted by:

Dr. S. Alan Stern, Principal Investigator
Space Sciences Division
Southwest Research Institute
San Antonio, Texas

March 22, 1994

SOUTHWEST RESEARCH INSTITUTE
Instrumentation and Space Research Division
6220 Culebra Road, San Antonio, Texas 78238
(512) 684-5111 • FAX (512) 647-4325

INTRODUCTION

This is the March 1994 Semi-Annual report for NAGW-3023 (SwRI Project 15-4971), *Studies of Extra-Solar Oort Clouds and the Kuiper Disk. (S.A. Stern, PI).*

We are conducting research designed to enhance our understanding of the evolution and detectability of comet clouds and disks. This area holds promise for also improving our understanding of outer solar system formation, the bombardment history of the planets, the transport of volatiles and organics from the outer solar system to the inner planets, and to the ultimate fate of comet clouds around the Sun and other stars. According to "standard" theory, both the Kuiper Disk and Oort Cloud are (at least in part) natural products of the planetary accumulation stage of solar system formation. One expects such assemblages to be a common attribute of other solar systems. Therefore, searches for comet disks and clouds orbiting other stars offer a new method for inferring the presence of planetary systems.

Our three-year effort consists of two major efforts: (1) observational work to predict and search for the signatures of Oort Clouds and comet disks around other stars; and (2) modelling studies of the formation and evolution of the Kuiper Disk (KD) and similar assemblages that may reside around other stars, including β Pic. These efforts are referred to as Task 1 and 2. The main collaborators with PI Stern in Task 1 are CoIs Drs. David Weintraub (Vanderbilt U.) and Mike Shull (U. Colorado). The main collaborator in Task 2 is CoI Dr. Glen Stewart (U. Colorado).

RECENT PROGRESS

Task 1: Observations Studies of Comet Disks and Clouds

We have recently completed 3 new observing runs at the JCMT, CSO, and IRAM submm telescopes to study one of the best IRAS IR-excess comet cloud candidates, α PsA (Fomalhaut). These runs have resulted in an exciting detection which we summarize as follows:

- S.A. Stern (Southwest Research Institute, San Antonio), M.C. Festou (CNRS, Toulouse), and D.A. Weintraub (Vanderbilt University, Nashville) report mapping observations of 20-21 February 1993 reveal 1.3mm continuum emission in a broad, disk-like region around the nearby, main sequence star α PsA (Fomalhaut A3V; D=6.7pc). The observations supporting this discovery were made using the 7-channel MPIfR bolometer of the IRAM 30-m telescope on Pico Veleto, Spain, with a HPBW at 1.3mm of 12". The emission geometry appears to be a tilted disk with the PA of the major axis near 100 deg and an aspect ratio of near 2:1; the major axis emission exceeds 18 mJy at the 190 AU contour. Additional emission may be present at larger distances. The peak 1.3mm emission detected is 35 mJy, centered on the line of sight to the star. The emission is ascribed to an assemblage of cold, orbiting dust grains around α PsA. Although IRAS revealed that Fomalhaut is an IR excess source, these observations constitute the first map of this extended, disk-like emission. Thus, after β Pic (also A3V), α PsA is the first disk around a main sequence star to be mapped in

millimeter-wave thermal emission. Fomalhaut's 2.5 times closer distance to Earth make it an ideal object for intensive study.

An important implication of this work is that the disk around Fomalhaut, like β Pic's, has not yet reached a steady-state and is still undergoing fast collisional evolution hundreds of millions of years after the parent star reached the main sequence.

These results were initially published in IAU Cicular 5732, and the *BAAS*, and is now in press for *Nature*. Observing proposals to extend this work to other stars, and to make a second-generation study of Fomalhaut has been written and accepted to IRAM and ESO/SEST for 1994. A preprint of the *Nature* paper on Fomalhaut is included in Appendix A of this report.

In addition to the Fomalhaut detection, we have also made important progress on several other sources. These are described in a second paper written this year, which is also attached as Appendix B. That paper (Weintraub & Stern 1994) has been submitted to the *Astronomical Journal*. It reports new evidence supporting a gap in the Vega disk, supporting evidence for the Fomalhaut disk, and in addition, presents the first submm evidence for an extended dust structure at β Uma. Most importantly, this paper also makes a strong argument that point-bolometry submm observations are prone to zero-point offset errors, and therefore that many such observations made by the community may have inadvertantly incurred significant errors. For the future, we stress that only mapping observations should be made when studying resolved disks.

Task 2: Collisional Modelling of the Kuiper Disk

We have now completed the first model of collision rates of the Kuiper Disk, and presented the initial results produced by this model at the AAS/Division of Planetary Sciences Meeting in October 1993. As a part of this presentation, an abstract was also published in the *BAAS*.

The findings of this research bear directly on the ancient and present-day structure of the Kuiper Disk. In particular, we show: (i) that the present-day disk inside $\sim$ 75 AU is probably the relic of a more massive, original disk; (ii) that the Kuiper Disk beyond $\sim$ 75 AU may be more significantly massive than previously recognized; and (iii) that the present-day rate of collisions in the Kuiper Disk may be detectable by dedicated observations using space infrared observatories.

We are now preparing a complete publication for *Icarus* which thoroughly describes the model and discusses our results in detail. In addition a popular paper (Stern 1994) has been written and accepted for *Astronomy* magazine describing the Kuiper Disk and our collisions work; this article (Appendix C) will appear on the cover of *Astronomy* in August 1994. An invited talk summarizing this work has been scheduled for June 3, 1994 at the Goddard Space Flight Center scientific seminar series.

RELEVANT NEW PUBLICATIONS

A Map of a Collisionally-Evolving Disk Around Fomalhaut (α PsA). S.A. Stern, M.C. Festou, and D.A. Weintraub, 1994. *Nature*, in press.

Chiron and the Kuiper Disk. S.A. Stern, 1994. *Astronomy* Magazine, in press.

A Reinterpretation of Millimeter Observations of Nearby IRAS Excess Stars. D.A. Weintraub and S.A. Stern, 1993. Submitted to *The Astronomical Journal.*

Collisions in the Kuiper Disk. S.A. Stern and G.R. Stewart, *Icarus*, in preparation 1994.

RELEVANT NEW PRESENTATIONS AND ABSTRACTS

A Tale of Two Disks. Lowell Observatory Colloquium. Flagstaff, Az. 17 July 1993.

Collisions in the Kuiper Disk. Division of Planetary Sciences Meeting. Boulder, Co. 19 October 1993.

Catching Small Waves on the Big Island: Submm Astronomy of Fomalhaut and Other Stellar Disks. S.A. Stern, San Antonio Amature Astronomical Association (SAAA), San Antonio, Tx. 10 September 1993.

The Discovery of a Disk Around Fomalhaut and It's Relation to The Kuiper Disk. Brown University. Geology Department Seminar. Providence, RI. 2 December 1993.

APPENDIX A

A Millimeter-Wave Map of the Collisionally-Evolving Disk Around Fomalhaut (α PsA)

(Stern, et al. 1994)

A Millimeter-Wave Map of the Collisionally-Evolving Disk Around Fomalhaut (α PsA)

S. Alan Stern
Space Sciences Department
Southwest Research Institute
6220 Culebra Road
San Antonio, TX 78238

[210]522-5127
alan@swri.space.swri.edu

Michel C. Festou
Observatoire Midi-Pyrénées
14 avenue E. Belin
F-31400 Toulouse, France

and

David A. Weintraub
Department of Physics and Astronomy
Vanderbilt University
Nashville, TN 37235

Submitted: 03 August 1993
Revised: 28 January 1994

Observations made by the 1983 IRAS spacecraft mission revealed that several main-sequence stars emit excess far-infrared radiation above their photospheric blackbody curves[1], indicating the presence of cold, solid grains in orbit around these stars[2]. Observations at visual wavelengths of one of these stars[3], β Pictoris, also revealed scattered light from a circumstellar disk extending ~1000 astronomical units (AU) from the star. Various workers[4,5,6,7,8] have persuasively argued that the loss time for the orbiting dust detected by IRAS is short (typically 10^{7-8} yr) compared to the typical main-sequence age of many IR excess stars (typically $10^{9-9.5}$ yr), and that these short loss times strongly imply the presence of an embedded population of larger parent bodies undergoing present-day collisions which produce the observed, transient population of small grains. We report here the first mm-wavelength map revealing extended thermal emission from dust around a main-sequence IR excess star, Fomalhaut. This map is clear evidence that the IR excess first detected by IRAS is extended, and that the rate of collisions of parent bodies leading to the dust emission signature is larger than previously recognized.

Electromagnetic radiation from a typical main-sequence star is very nearly that of an ideal, isothermal blackbody. Each main-sequence stellar type has a unique temperature, characteristic of the thin, photospheric region from which it emits most of its light. From measurements at visual wavelengths, one can determine the photospheric temperature of a star and thereby directly calculate the amount of emission the star will produce as a function of wavelength. Certain stars, specifically those in the process of either forming or dying, are commonly surrounded by substantial amounts of fine-grained cold material. During the ≈90% of a star's lifetime which it spends on the *main-sequence*, however, the stellar environment is normally free of microscopic dust particles. The IR excess stars discovered by IRAS are main-sequence stars character-

ized by as much as an order of magnitude more emission at far-IR wavelengths than predicted from their photospheric blackbody profiles. The most likely source for this far-IR excess radiation has convincingly been shown to be orbiting dust grains heated by the star[2]. Because the dynamical lifetime of this dust is short, an underlying population of comets or asteroids undergoing mutual collisions is implied. As such, it is widely believed that studies of these far-IR excess systems provide information regarding the processes and time scales involved in solar system formation and/or evolution.

Although no successor far IR space mission to IRAS has yet flown, Chini, et al.[9,10] and Zuckerman and Becklin[7,8] have pioneered the use of the longer-wavelength submillimeter and millimeter groundbased windows to make important advances. However, previous work on IRAS IR excess stars such as theirs has relied on point-flux observations made along the lines of sight to these stars. With the advent of bolometer arrays in the millimeter wavelength range, it has now become possible to *map* the emission around these stars, and therefore further refine knowledge about the spatial distributions and masses of their cool dust structures. We made observations of Fomalhaut (α PsA; A3V; D=6.7 pc) at the IRAM (Institut de Radio Astronomie Millimétrique) telescope at Pico Veleta, Spain on 19-20 February 1993 UT, at an effective wavelength of 1.3 mm, and in excellent, very dry weather. We used the Max-Planck-Institut für Radioastronomie (MPIfR) 7-channel bolometer[11]. The seven beams of the MPIfR bolometer are arranged in a hexagon surrounding a central channel. At 1.3 mm, each beam operates with a diffraction-limited half power beam width (HPBW) of 12 arcsec, corresponding to 80 AU at Fomalhaut. The center-to-center separation of the bolometer beams is 22 arcsec (150 AU). Since most of the observed flux in any astronomical millimeter-wave bolometer measurement is thermal emission from Earth's 100 K atmosphere, we adopted the standard procedure of using a chopping secondary mirror to remove the telluric sky signal. The secondary was set to produce a chop throw of 45 arcsec at a chop frequency of 2.0 Hz. For our flux calibrator, Uranus, we adopted a 1.3

mm brightness temperature of 97.5 K[12,13]. Observations of Uranus were used to compute a system noise equivalent flux density (NEFD) of 80 mJy $Hz^{-1/2}$ $channel^{-1}$, in good agreement with that quoted (90 mJy $Hz^{-1/2}$ $channel^{-1}$) in the nominal observing performance specifications for the array.

Accurate pointing for each observation of Fomalhaut was ensured by offsetting to the position of the star after using a Gaussian fit routine to center and focus on the nearby (1 deg north) source 2255−282, whose position has been well-established[14]. Routine pointing checks revealed reliable performance with < 3 arcsec (2-axis rms) pointing errors. Three, 3×2 arcmin maps were obtained by raster scanning the array over the field around Fomalhaut at an angular velocity of 4 arcsec/sec, with cross-scan direction steps of one-half beam (6 arcsec). An unsmoothed, S/N-weighted coaddition of our three maps is shown in Figure 1. The 120 × 80 arcsec area shown in Figure 1 is the fully-sampled portion of the full (180 × 120) arcsec map areas; partial sampling near edges occurs because only some of the seven beams are on the map area along its edges.

Figure 1 reveals a roughly elliptical emission region centered on the 1993 position of Fomalhaut. The peak 1.3 mm emission detected toward Fomalhaut is 32±12 mJy, along the line of sight to the star. The 1σ error level of 12 mJy per beam in our data (taken at high airmass but in optimal weather) compares well with the predicted sensitivity of 8 mJy. The total flux detected above the 18 mJy contour surrounding Fomalhaut is 305±80 mJy (a 3.8σ detection of the extended emission). Owing to its proper motion, Fomalhaut has moved 16.8 arcsec since 1950.0. The center of the 32 mJy isophote surrounding the peak emission corresponds to within 0.5 arcsec in Right Ascension and 6 arcsec in Declination of the proper motion corrected position of Fomalhaut. At the signal to noise of our data, this one-half beamwidth offset is not statistically significant. The close correspondence between the emission peak in the map and the position of the star is strong evidence that we detected radiation from

dust around Fomalhaut, rather than a randomly superimposed background source.

It is important to point out that this extended emission is not due to Fomalhaut's photosphere. This is because the flux from Fomalhaut's 8800 K photosphere is a point source 10^4 times smaller than the IRAM beamsize, with a predicted flux of < 1 mJy, and is not detectable with present-day mm-techniques. As such, we conclude that the mm emission region mapped around Fomalhaut is due to thermal emission from the dust surrounding this main-sequence IR excess star. With this detection, the dust assemblage surrounding Fomalhaut becomes an important analog to that surrounding the well-known IRAS IR excess star β Pictoris (A5V, D=16.7 pc), which was mapped in *scattered* light almost a decade ago[3]. Our 1.3 mm map confirms and significantly extends earlier results,[5,7,8,9,10,17,18] which inferred, but did not directly detect extended emission around Fomalhaut. The 18 mJy contour in Figure 1 suggests that the emission source likely extends at least 190 AU from Fomalhaut in the east and west directions, but appears to be unresolved in the N-S direction. On the sky, the detected 18 mJy emission contour subtends 1 arcminute in the E-W direction. Although the S/N per beam of this detection is too low to make strong quantitative statements about the geometry and total flux density of the extended source, future observations with more integration time should make this possible. More sensitive observations should also reveal whether the disk is more extended at lower flux levels than we can reliably measure in this first-detection.

As noted above, all past measurements of submillimeter and millimeter wavelength emission along the line-of-sight to Fomalhaut have all been made using single channel bolometers making point-observations. The net flux measured by this technique is the difference between the flux measured along the line-of-sight and the flux measured at the chop position, which is implicitly assumed to be zero. With this technique Chini et al.[9,10] obtained 7.3 ± 2.2 mJy at 1.3 mm with a 12 arcsec HPBW and a 30 arcsec chop throw at IRAM. The same workers later detected three times as much flux, 21 ± 2.5

mJy, at 1.3 mm with a 24 arcsec HPBW and a 70 arcsec chop throw at the 15m SEST (the Swedish-ESO Submillimeter Telescope) observatory.

Our map reveals a flux along the central line of sight to Fomalhaut that appears to be higher than but not inconsistent with the extended emission region detected in past non-mapping observations[7,8,9,10]. The additional flux we detected is present outside the central region. The extended nature of the Fomalhaut emission apparently revealed by the 1.3 mm map suggests that some of the point-observations of Fomalhaut made in the past may have "chopped away" and/or missed flux outside their line-of-sight beams. This hypothesis is supported by the fact that Chini, et al. found a larger flux[10] in their larger beam experiment at SEST, which is consistent with their IRAM measurements only if Fomalhaut is extended at 1.3 mm compared to the 12 arcsec HPBW of the IRAM measurement. Given this finding, we suggest that disk properties of Fomalhaut and other IR excess stars studied by point-bolometer work at submm/mm wavelengths require re-evaluation using mapping techniques. This finding has recently been described in detail[19].

To estimate the total dust mass detected in the disk around Fomalhaut revealed in Figure 1, we assume the dust grain opacity is described by a power law in frequency[20]

$$\kappa_\nu = \kappa_o \left(\frac{\nu}{\nu_o} \right)^\beta , \tag{1}$$

where κ_o is the value of the dust grain opacity at a reference frequency ν_o. Next, following Sandell and Weintraub[21], we use Eqn(6) of Hildebrand[20] to write an expression for the dust mass, M_{dust}:

$$M_{dust} = 3.76 \times 10^{20} \left(\frac{1200}{\nu} \right)^{3+\beta} F_\nu \, (e^{0.048\nu/T_{dust}} - 1) \, D^2 \text{ grams}, \tag{2}$$

where ν is given in GHz, F_ν in mJy, T_{dust} in K, the distance D in pc, and we adopted $\kappa_o = 10.0$ cm^2 g^{-1} at $\nu_o = 1200$ GHz (i.e., 250 μm). This expression assumes that the emission from dust at 1.3 mm is optically thin, but does not assume the spectrum

is on the Rayleigh-Jeans tail. The optically thin assumption is strongly supported by previous IRAS and millimeter studies of Fomalhaut[2].

For an integrated flux density of 305 mJy and a typical dust temperature of 43 K (expected 100 AU from Fomalhaut; $L_* = 6.7 L_\odot$), we estimate a dust mass of $M_d = 2.3 \times 10^{26} \times 5.2^{\beta}$ g. We use $\beta = 0$ and $\beta = 2$ to obtain minimum and maximum estimates of M_d. This gives the range $4.4 \times 10^{26} < M_d < 1.2 \times 10^{28}$ g, or $\approx$ 0.07-2 M_{earth}. Variations in the dust temperature between 30 and 100 K (as appropriate for distances of 20 to 200 AU do not change the results by more than a factor of 2. These mass estimates indicate that the mass of Fomalhaut dust detected at 1.3 mm is at least 10^5 more than in our own solar system's interplanetary dust cloud[22].

Now consider the timescales for loss of dust from the Fomalhaut system. The dominant dynamical loss mechanism beyond ~60 AU is Poynting-Robertson (P-R) drag. P-R drag limits the lifetime of low-eccentricity grains to $\approx 1 \times 10^6 \; R_{100}^2 r \rho_{2.0}$ yr, where R_{100} is the astrocentric semi-major axis in units of 100 AU, r is the grain radius in microns, and $\rho_{2.0}$ is the grain density in units of 2.0 g cm^{-3}. For the estimated stellar age of Fomalhaut, $2 \pm 0.7 \times 10^8$ yr,[23] the P-R lifetime of 30 micron grains 100 AU from Fomalhaut is 0.15 times the present age of Fomalhaut. Smaller grains are removed even faster. Even at 200 AU, the P-R lifetime for 30 micron grains against P-R drag is less than the estimated age of the star. For millimeter-sized particles the P-R transport lifetime can approach the age of Fomalhaut at 200 AU. However, using a robust particle in a box model[6,24,25], it is possible to show that collisions between mm-sized grains in the system will remove these particles on orbits with eccentricities exceeding 1% on timescales of 10^{6-7} years, even at 200 AU. The short grain lifetimes indicated by these simple calculations provide strong circumstantial evidence for recent dust production around Fomalhaut, at least for the region inside 200 AU of interest here.

Conservatively taking 5×10^7 years as a relevent dust loss timescale, the steady-

state production rate of dust needed to supply the mass of the *observed* Fomalhaut disk implies a total loss of 2×10^{27} to 5×10^{28} g (0.3-8 M_{earth}) over the age of the star. Since 1.3 mm observations are not sensitive to either the mass locked up in large bodies (which have low surface area to mass ratios) or in micron-sized grains (which are inefficient emitters at mm wavelengths), these dust loss and total disk mass estimates represent lower limits.

Because the lifetime of the observed dust is short compared to the age of Fomalhaut, it is natural to invoke an embedded population of planetesimals undergoing collisions as a mechanism to produce the observed dust. If we assume a typical instantaneous dust mass of $\sim 10^{27}$ g and a dynamical lifetime of 5×10^7 yr, a dust production rate of 2×10^{19} g/yr is implied. This is equivalent to 25 to 100 comet Halley masses (each $\approx 1 - 4 \times 10^{17}$ g) being ground up each year. This rate of collisions is $10^2 - 10^3$ times the rate of cometary collisions occuring in the present-day Kuiper Disk surrounding the Sun[24,25]. Recognizing the high rate of collisions implied by the dust resupply rates required at Fomalhaut, we suggest that its disk is still rapidly evolving from its formation state toward a less massive remnant disk like our Kuiper comet belt. Whether planets have already formed or are now accumulating from the colliding bodies around Fomalhaut is an exciting area for future investigation.

Figure Caption

Fig. 1. A coadded, 120x80 arcsec, 1.3 mm map of the region around Fomalhaut made at IRAM is shown here; north is at the top, east to the left. The edges of the larger, 3x2 arcmin maps are not displayed because they were not uniformly sampled, as the central region is (see text). Fomalhaut's 1993 position is indicated by the small cross at the center. The icon at the upper right represents the IRAM 1.3 mm beam size (12 arcsec HPBW). There is no significant signal in the map below -1σ (-12 mJy); thus the noise level is well illustrated with the $\pm 1\sigma$ ($+12$ mJy = solid line; -12 mJy = dashed line) contours. Higher contours are drawn at 0.5σ intervals (18, 24, and 30 mJy). The 0 mJy contour is shown with a dashed line to illustrate the flatness of the subtracted baseline. The three prominent peaks near the map center are separated by intervals of $\sim$22 arcsec, which is close to but not the same as the spacing of the bolometer detectors; further, these three peaks do not form the hexagonal pattern of the detectors, and are not in the bolometer scan direction. We conclude they are real.

The map was made in azimuth/elevation coordinates over 2.7 hours. During this 2.7 hours, the airmass of Fomalhaut ranged between 2.5 and 3.1. Proper pointing was verified between maps. The sky transmission was measured three times using a standard skydip procedure. This revealed an essentially constant 1.3 mm zenith optical depth of $\tau_{1.3} = 0.13 \pm 0.01$ during the observations. The instrument was operated at highest gain for maximum sensitivity.

The three maps of the Fomalhaut area were individually cleaned, reduced to RA/Dec coordinates, and converted to calibrated flux using the IRAM NOD2 software package[15,16]. Single pixel data glitches (or 'spikes') above the 3-σ level were removed. The three co-registered maps were co-added and a fitted background plane was removed. This slightly tilted background plane was constrained not to remove flux at the location of Fomalhaut.

The prominant feature at the center of the map is the extended emission feature

resulting from Fomalhaut's extended dust ensemble. Minor peaks in the map with lower fluxes and much smaller solid angles are due to either statistical noise and/or map edge effects.

References

1. Aumann, H.H., F.C. Gillet, C.A. Beichmann, T. de Jong, J.R. Houck, F.J. Low, G. Neugebauer, R.G. Walker, and P.R. Wesselius *Astrophys.J.* **278**, L23-27 (1984).

2. Backman, D.E., and F. Paresce. In *Protostars and Planets III* (Eds. Levy, E., Lunine, J.I.) (Univ. of Az. Press, Tucson, Az, 1993) 1253-1304.

3. Smith, B.A., and R.J. Terrile *Science* **226**, 1421-1424 (1984).

4. Weissman, P.R. *Science* **224**, 987-989 (1984).

5. Harper, D.A., R.F. Lowenstein, and D.A. Davidson, *Astrophys.J.* **285**, 808-820 (1984).

6. Stern, S.A. *Icarus* **84**, 447-466 (1990).

7. Zuckerman, B., and E.E. Becklin, In *Submillimetre Astronomy* (Eds. Watt, G.D. and Webster, A.S.) 147-153 (Klüwer, Dordrecht, 1993).

8. Zuckerman, B., and E.E. Becklin, *Astrophys.J.* **414**, 793-802 (1993).

9. Chini, R., E. Krügel, and E. Kreysa *Astr. Astrophys.* **227**, L5-11 (1990).

10. Chini, R., E. Krugel, B. Shustov, A. Tutokov, and E. Kreysa, *Astr. Astrophys.*, **252**, 220-228 (1991).

11. Kreysa, E., R. Lemke, C.G.T. Haslam, and A.W. Sievers *Astr. Astrophys.* (1994), in press.

12. Griffin, M.J. *et al. Icarus* **65**, 244-258 (1986).

13. Orton, G.S. *et al. Icarus* **67**, 289-301 (1986).

14. Sandell, G. in preparation (1994).

15. Haslam, C.T.G. *Astr. Astrophys. Suppl.*, **15**, 333-350 (1974).

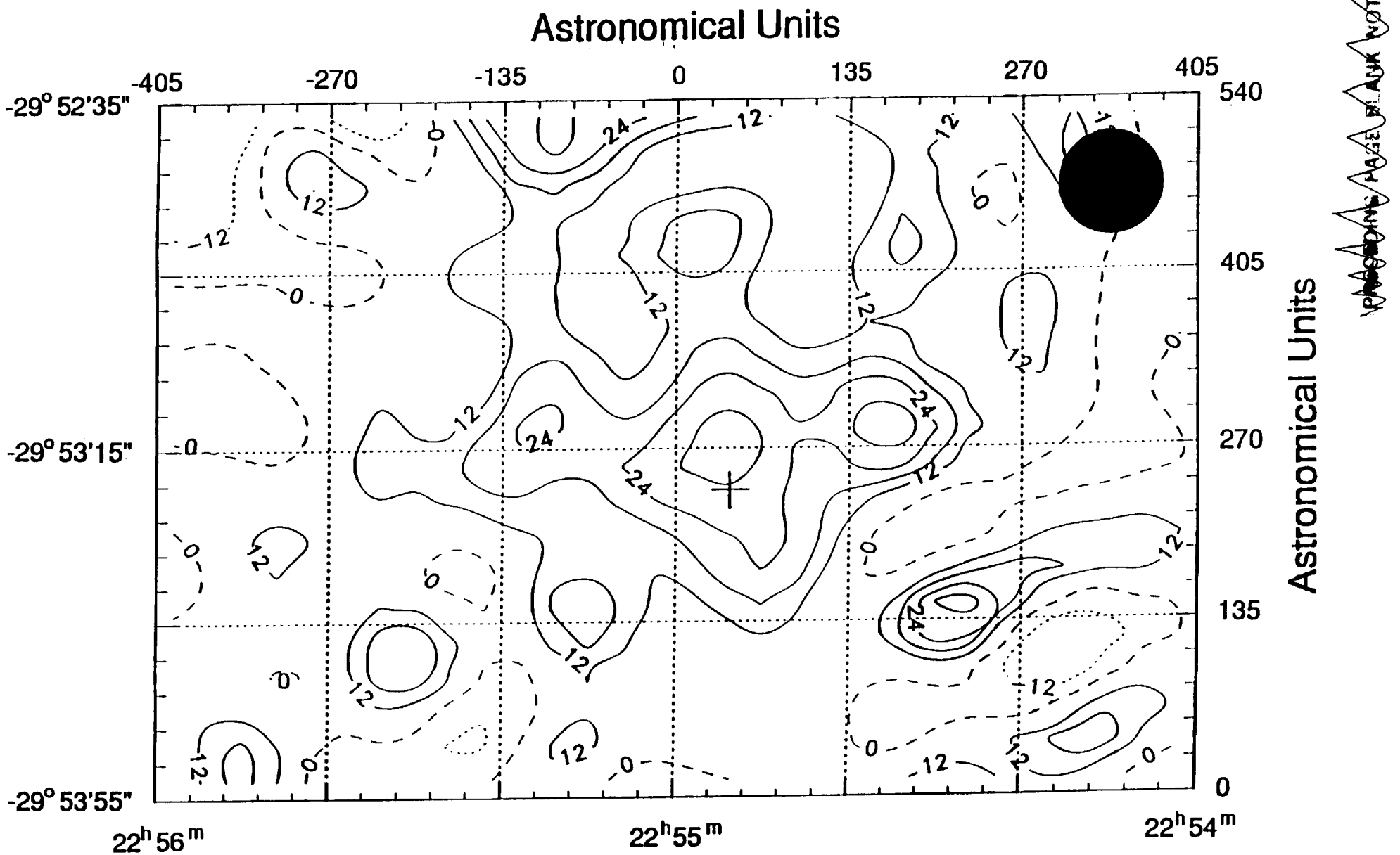
Astronomical Units
-405
-270
-135
0
135
270
405
-29° 52'35"
-29° 53'15"
-29° 53'55"
22h 56m
22h 55m
22h 54m
540
405
270
135
0
Astronomical Units

16. Salter, C.J. *IRAM Preprint*, 84 (1986).

17. Gillet, F.C. In *Light on Dark Matter* (Ed. Israel, F.P.) 61-69 (Reidel, Dordrecht, 1986).

18. Aumann, H.H. In *The Infrared Spectra of Stars* (Pergamon, New York, 1990).

19. Weintraub, D.A. and S.A. Stern, *Astr.J.*, submitted (1994).

20. Hildebrand, R.H. *Quart. J. Roy. Astron. Soc.* **24** 267-282 (1983).

21. Sandell, G. and D.A. Weintraub, *Astr. Astrophys.*, submitted (1994).

22. Sykes, M.V., et al. In *Asteroids II* (Eds., Binzel, R.P., Gehrels, T., Matthews, M.S.) 336-368 (1989).

23. Green, E.M., P. Demarque, C.R. King *The Revised Yale Isochrones and Luminosity Functions*, (Yale Univ. Obs., New Haven, 1987).

24. Stern, S.A., and G.R. Stewart. *B.A.A.S.* **26**, (1993).

25. Stern, S.A., and G.R. Stewart. *Icarus*, submitted (1994).

ACKNOWLEDGMENTS. We thank the staff of the IRAM observatory for their assistance with the observations. We particularly thank A. Sievers for assistance with the IRAM NOD2 bolometer image recovery package. D. Backman, J. Bally, and M. Duncan provided helpful comments on this manuscript. Gören Sandell kindly provided us with a list of mm pointing sources in advance of its publication. This work was supported by the NASA Origins of Solar Systems program under NAGW-3023 and travel grants from the NRAO (for SAS) and IRAM (for MFC).

APPENDIX B

A Reinterpretation of Millimeter Observations of Nearby IRAS Excess Stars

(Weintraub & Stern 1994)

A REINTERPRETATION OF MILLIMETER OBSERVATIONS OF NEARBY IRAS EXCESS STARS

David A. Weintraub[1,2] and S. Alan Stern[2,3]

[1] Department of Physics and Astronomy
Vanderbilt University
Nashville, TN 37235
(615) 322-5034
david@ttau.phy.vanderbilt.edu

[2] Visiting Astronomer
CalTech Submillimeter Observatory
Mauna Kea, Hawaii

[3] Space Sciences Department
Southwest Research Institute
6220 Culebra Road
San Antonio, TX 78238
(210) 522-5127
alan@swri.space.swri.edu

19 Pages
02 Figures
05 Tables

Submitted: 01 December 1993
Revised: 02 February 1994

ABSTRACT

We analyze new and previously published 1300, 870 and 800 μm, single-element bolometer observations of Vega (α Lyr), Fomalhaut (α PsA), ϵ Eri, τ^1 Eri and β Leo. We show that these data are consistent with models in which the dust disks around these stars are larger than the radio telescope beams with which they were observed; thus these disks may be many hundreds of AU in radius or larger. Our interpretation of the submillimeter/millimeter measurements of these stars also indicates that for some IRAS IR excess stars the assumption that there is no astrophysical flux in the OFF beams, when using the standard ON-minus-OFF chopping technique and the chop distance is less than 1000 AU, may be incorrect. Therefore, for IRAS IR excess stars within ~20 pc, virtually all submillimeter/millimeter chopping observations with chop throws less than 100″ may have subtracted away some or most of the flux associated with their circumstellar disks. Finally, we present new 1300 μm continuum observations of Vega made with chop throws of 500 AU and 1000 AU. These data are consistent with an interpretation in which Vega has a disk that is at least 1000 AU in radius; this disk could have a region with much less material per beam area near 500 AU than at both 100 AU and 1000 AU, corresponding to a gap at the orbital distance of α Lyr B. The observations of Vega are also consistent with the assumption that the circumVega dust structure is unresolved. Thus, these new data very effectively illustrate that the "standard" model of small, unresolved, dust structures around main-sequence IRAS IR excess stars is not unique. Maps of IRAS IR excess stars, which soon will be available from submillimeter/millimeter array detectors, will determine whether the paradigm shift we propose will occur.

1. INTRODUCTION

Virtually all published submillimeter/millimeter observations of IRAS excess main-sequence (Vega-type) stars have fairly low signal-to-noise ratios (Chini *et al.* 1990, hereafter Chini90; Chini *et al.* 1991, hereafter Chini91; Zuckerman and Becklin 1993, hereafter ZB93; Mannings & Emerson 1993). In interpreting these observations, these and other authors have assumed that the "standard" model for IRAS IR excess stars is correct. In the standard model, the circumstellar dust source detected in thermal emission at long wavelengths is assumed to be fairly small. Consequently, the positions chosen for the OFF (or sky) beam measurements, 30″ to 70″ from the stars sould include no astrophysical flux.

In this paper we postulate a different model for the environments of IRAS IR excess stars, one in which the circumstellar dust structures are much larger. As a test of this hypothesis, we undertook a small program of 1300 μm continuum flux observations of several Vega-like stars, with an emphasis on observations of Vega itself, to further investigate the size of their disks. We argue that the alternative model — large disks — is an equally reasonable interpretation of the existing data, including the new observations of Vega. Dust in

these large disks could be generated by collisions among comets. Models of debris disks generated by Kuiper disks of comets predict that these disks should peak 300 to 3000 AU from the parent star (*e.g.*, Stern *et al.* 1991). Thus, the likely circumstellar dust structures are much larger than envisioned for environments in which much of the dust is produced perhaps through asteroid belt collisions. These larger dust structures would be resolvable by groundbased submillimeter/millimeter telescopes.

In order for the reader to follow our discussion of the relative merits of the standard model versus our large disk model, we first describe (in §2) the procedures used by us and other observers to measure submillimeter and millimeter flux densities. Then we examine in §3 the new and published results for Vega, for which data has been collected by different observers at three different telescopes, to illustrate in detail the consistencies and inconsistencies within the complete body of data for one IRAS IR excess star. We then expand our discussion in §4 to analyze existing photometry for Fomalhaut, ϵ Eri and τ^1 Eri. We summarize our results and our thesis in §5.

2. OBSERVATIONS

2.1 The Observing Program

The observations we report herein were obtained in April 1993 on the 10.4m Caltech Submillimeter Observatory telescope (CSO), on Mauna Kea, Hawaii. We used a ^{3}He-cooled, single-channel bolometer, equipped with a 1300 μm filter and iris. During this observing run, we measured the half-power-beam-width (HPBW) to be $\sim$30″. The measured noise equivalent flux density (NEFD) ranged from $\sim$240 to 360 mJy Hz$^{-1/2}$. Sky cancellation was achieved with a chopping secondary. Using Uranus and several bright submillimeter standards with well established positions, we established that the CSO pointing was better than $\pm$3″, even after slewing the telescope several tens of degrees. Source observations were made by offsetting to 1993.3 positions after using a simple five-point routine to peak up on nearby sources (K3-50 for Vega; $+2255-282$ for Fomalhaut; 3C273 for β Leo). We used chop throws of 500 AU and 1000 AU for Vega (62″ and 123″, respectively), and 1000 AU for Fomalhaut (150″) and β Leo (83″). All chops were made in azimuth at $\sim$10 Hz. Basic data for our three target stars, as well as for two other stars discussed in this paper, are listed in Table 1.

Variations in the sky transmission were tracked using the CSO 226 GHz narrow band sky monitor. As is common practice, we assumed the narrow band optical depth, τ_{CSO}, was linearly proportional to the 1300 μm broad band optical depth according to the relationship $\tau_{1.3} = C_{1.3}\tau_{CSO}$, where $\tau_{1.3}$ is the 1300 μm zenith optical depth and the $C_{1.3}$ is the proportionality constant between the narrow and broad band optical depths. We determined $C_{1.3}$ from observations of Mars and Uranus, for which the same-epoch 1300 μm temperatures and flux densities (Griffin *et al.* 1986; Orton *et al.* 1986) were determined using James Clerk

Maxwell Telescope (JCMT) system software. Additional photometric checks were made of K3-50, 3C273 and CRL 618.

2.2 Standard Chopping Protocol

We observed according to standard procedures for chopping observations. Each observation consisted of a specified number (40, 50, or 100) of 9 s data cycles collected consecutively. Different observations are separated in time and by calibration and pointing checks. During the first 4.5 s of each cycle, the secondary chops back and forth at 10 Hz from the first positive beam (on the position of the star) to the second negative beam (presumed empty sky) position (Fig. 1). Before the second half of each cycle, the telescope nods one chop throw distance in azimuth. This motion puts the source in the second negative beam, and correspondingly places the presumed empty sky position (equal distant on the other side of the source position) in the second positive beam. The chopping pattern is then repeated. A typical observation consist, for example, of 100 ON and OFF pairs. In each pair the net ON flux (ON the source) is the signal in the first positive beam minus the signal in the second negative beam. The net OFF flux (OFF the source; on the sky) consists of the signal in the first negative beam minus the signal in the second positive beam. The net source flux is the net ON flux minus the net OFF flux.

In chopping observations, OFF positions include thermal flux from local background and telluric foreground sources. For the results to be valid, however, this position also must be empty of measurable flux from astrophysical sources. If the telescope were chopping onto an extended source (Fig. 1), a background plateau of astrophysical flux would exist in both the ON and OFF signals. In this case, since the astrophysical flux density at the reference position is not actually zero, such a measurement will not provide an accurate measure of the *absolute* flux of the source at the position of the peak. Instead it will yield the relative flux of the source *above* the background plateau.

2.3 Control Observations

In a set of control observations during an unrelated 1300 μm continuum program on the JCMT in May 1993, we observed a region of sky void of any known (*i.e.* detectable) astrophysical sources. In a set of 83, 10 s ON-minus-OFF pairs, using a 60″ chop at 7.812 Hz, the integrations rapidly converged toward a signal level of zero. The noise level integrated down with the square root of increasing observing time as predicted from the system NEFD. We obtained 4 ± 13 as our final measurement of "blank sky." In comparable integration times as those used in the CSO observations, we also obtained dependable detections of a known faint point source (Pluto, 10-15 mJy; Altenhoff *et al.* 1988, Stern *et al.* 1993). In numerous 1000 s observations of Pluto with both the JCMT and IRAM (Institut de Radio Astronomie Millimetrique, Pico Veleta, Spain), we

never obtained a zero or negative flux. These control experiments convincingly demonstrate that, in fairly long integrations, the chopping technique does yield signal levels consistent with zero if no source is present, and a positive signal if a very faint point source is placed in the ON beam. Therefore, signal levels that are larger than the statistical errors and that deviate to either positive or negative levels should be considered as suggestive of of true astrophysical flux *differences* between the net signals in the ON and OFF beams.

As part of our CSO program, we observed β Leo. This star is an IRAS IR excess star with only a small 100 μm IRAS excess (0.63 Jy; Backman and Paresce 1993). From this excess we predict a 1300 μm flux density of only 0.02 mJy to 3.7 mJy. Thus, β Leo serves as a good test star for detecting (or not detecting) extremely faint sources. We are not aware of any previous submillimeter bolometry for this source. We made two independent, 900 s integrations at 1300 μm along the line of sight to this star (Table 2a). The sum of these observations is a weakly positive signal, 2.5 $\pm$ 7.1 mJy, which is formally indistinguishable from zero ($\leq$ 21.3 mJy; Table 2b) and which is consistent with our predictions.

3. VEGA

3.1 Background

Vega is the prototype IRAS IR excess star (Aumann *et al.* 1984). The flux density detected toward Vega by IRAS pointed observations exceeds that predicted for its 9700 K photosphere by more than an order of magnitude: 8.2 $\pm$ 0.5 Jy at 60 μm, and 7.1 $\pm$ 0.8 Jy at 100 μm. This corresponds to an isothermal 89 K far-infrared source. The intrinsic 60 μm diameter of Vega is 29″ (230 AU; Gillett 1986); however, this is not the limiting outer diameter since unknown amounts of cool dust might lie undetected outside these regions. Because the 60 μm IRAS field of view at Vega was 120″ $\times$ 300″ (1000 $\times$ 2500 AU), the true source size could be substantially larger than the value given above.

Backman and Paresce (1993) point out that dust at 30 K would be located beyond 1000 AU from Vega, and that the emission peak of this cold dust would be beyond the long wavelength cutoff of the IRAS 100 μm detectors. However, ZB93 interpret multiposition 800 μm chopping observations of Vega and Fomalhaut as evidence that these stars do not have any dust too distant to have been detected by IRAS.

The dust clouds around Vega and other main-sequence IRAS IR excess stars are most likely evidence of active collisional processes in circumstellar disks. This part of the paradigm is widely accepted because particle loss processes such as radiation pressure, sublimation and Poynting-Robertson drag are sufficient to sweep at least the inner systems ($R < 100$ AU) clean of dust in only a few times 10^5 yr. Even at 1000 AU, mass loss occurs on time scales at least an order of magnitude smaller than the 4×10^8 yr age of Vega (Green *et al.* 1987). Similar arguments are easily made for most other IRAS IR excess stars.

3.2 Observations

The CSO results for Vega are presented in Tables 2a and 2b. The calibrated flux densities were obtained after examining and correcting the raw data for cosmic ray events. Cosmic ray events are often seen in submillimeter photometry work and the most energetic of these are easily identified in strip chart recordings and in individual ON-minus-OFF pairs stored in the data records. In this first stage of analysis, based on inspection of the strip chart recordings and the data numbers recorded for the ON-minus-OFF pairs, we identified two data points (out of 360) in the 500 AU chop set and one (out of 440) in the 1000 AU chop set that appear to be obvious cosmic ray events. Further checks (see below) were done to test this assumption. These three points were removed from the data sets before the initial calibrations. The individual runs were calibrated separately in order to examine the consistency of the data and to look for any patterns that might exist as a function of the chop position angle. Two patterns are clear, albeit all at low signal-to-noise levels: all the data sets obtained with a 500 AU chop throw are positive whereas the data sets obtained with a 1000 AU chop throw are sometimes positive and sometimes negative. No pattern is evident as a function of position angle.

To obtain our final results, the individual ON-minus-OFF data pairs were combined according to the following procedure. Each ON-minus-OFF pair was tagged with an airmass and optical depth. Then each pair was calibrated in mJy units and mean flux densities and standard deviations (σ) were computed for the 500 AU and 1000 AU data sets. Without despiking (keeping all 360 points), the derived flux density in the 500 AU chop set is 16.4 ± 6.1 mJy. We then examined the ON-minus-OFF pairs to determine a statistical test to determine the envelope of reasonable data pairs and to objectively, rather than subjectively, remove cosmic ray contaminated data. In the 500 AU chop data set, 358 of 360 ON-minus-OFF pairs lie within 3.4σ, 356 lie within 3.0σ and 349 lie within 2.5σ of the mean (the last grouping yields a flux density of 17.4 ± 5.1 mJy). Clearly, the data envelope is well defined and fairly tight. The two data points that appeared to be bad based on our visual inspection lie 7.0 and 5.5σ from the mean and lie far outside the envelope of the uncontaminated data set. The despiked signals are 18.7 ± 5.7 mJy (359 points included) and 17.0 ± 5.5 mJy (358 points included). The signal levels derived from the complete and despiked data sets are nearly identical; however, the absolute noise level is 10% lower after despiking and we believe the result 17.0 ± 5.5 mJy represents the best, most careful and most conservative analysis of the data. In the 1000 AU chop data set, all of the 440 data points are within 3.6σ of the mean (yielding the result -1.7 ± 5.4 mJy) and 439 of the points are within 2.8σ of the mean (yielding -2.6 ± 5.3 mJy). For the 1000 AU data set, only a single data point stands outside of the tight envelope. In this case, we believe -2.6 ± 5.3 mJy represents the best, most careful and most conservative analysis.

Our final results are presented in Table 2b. For comparison with these results, a compilation of past submillimeter and millimeter observations along the direct line of sight to Vega are presented in Table 3. Inherent in the presentation of the numbers in Table 2b and Table 3 is the assumption that the standard model is true. That is, we are assuming that the warm dust source that surrounds Vega is much smaller than the 1300 μm HPBWs of the CSO, JCMT or IRAM and that none of the OFF positions include astrophysical flux.

3.3 Dust Masses Estimated from the Millimeter Continuum Flux at 1300 μm

Following Hildebrand (1983), we assume the dust grain opacity is described by a power law in frequency

$$\kappa_\nu = \kappa_o \left(\frac{\nu}{\nu_o}\right)^\beta, \tag{1}$$

where κ_o is the value of the dust grain opacity at the specified frequency ν_o. Next, following Sandell and Weintraub (1994), we use equation (6) of Hildebrand to derive an expression for the dust mass, M_{dust}:

$$M_{dust} = 6.3 \times 10^{-8} \left(\frac{1200}{\nu}\right)^{3+\beta} F_\nu \, (e^{0.048\nu/T_{dust}} - 1) \, D^2 \;\; M_\oplus, \tag{2}$$

where ν is given in GHz, F_ν in mJy, T_{dust} in K, the distance D in pc, $\kappa_o = 10.0$ cm^2 gm^{-1} at $\nu_o = 1200$ GHz (250 μm), and M_{dust} is given in Earth masses. This expression assumes that the emission from dust at 1300 μm is optically thin. It does not assume, however, that the spectrum is on the Rayleigh-Jeans tail. In fact, if one measures flux at 1300 μm from dust with $T_{dust} \leq 50$ K, the Rayleigh-Jeans assumption is not justified. For observations of Vega at 1300 μm (230 GHz), we can rewrite M_{dust} as

$$M_{dust} = 4.13 \times 10^{-6} (5.2)^{3+\beta} F_\nu (e^{11.04/T_{dust}} - 1) \;\; M_\oplus. \tag{3}$$

Taking $F_\nu = 17.0$ mJy (from our 500 AU observations of Vega) and with $T_{dust} = 50$ K, we find 0.002 $M_\oplus$ < M_{dust} < 0.07 $M_\oplus$ where the lower limit applies for $\beta = 0$ (large grains) and the upper limit for $\beta = 2$ (small grains).

3.4 Is the Disk Resolved at 1300 μm?

If the Vega source is unresolved at 1300 μm and no astrophysical flux exists in the OFF beam positions used by either Chini90 or us, then a statistically significant discrepancy appears to exist between the 4.5 $\pm$ 1.5 mJy (3.0σ) measured by Chini90 at IRAM (12″ beam; 30″ chop) and the 17.0 $\pm$ 5.5 mJy (3.1σ) measured by us at CSO (30″ beam; 62″ chop). Apparently as much as 12 mJy may emanate from regions around Vega that are within the CSO beam and outside the IRAM beam, but lie within 24″ of Vega so as not to contaminate the OFF beam positions used at IRAM. Thus, if we accept that some discrepancy exists

between these two observations, we are led directly to a contradiction of the assumption that the source is unresolved in the IRAM beam. We must conclude that the IRAM measurement represents the flux density per 12″ beam, and not the total source flux density.

Based on this premise, we convert peak flux densities to integrated source flux densities by assuming that both the source and beam can be approximated by Gaussian functions. Then, following Chini *et al.* (1984), we can write

$$F_{total} = F_{beam,tele}\left[1+\left(\frac{\Theta_{major}}{\Theta_{\rm tele}}\right)^2\right]^{1/2}\left[1+\left(\frac{\Theta_{minor}}{\Theta_{\rm tele}}\right)^2\right]^{1/2}, \qquad (4)$$

where F_{total} is the total source flux density, $F_{beam,tele}$ is the measured flux density per beam at a given telescope, Θ_{major} and Θ_{minor} are the full-width-half-maxima (FWHM) of the source along the major and minor axes, and Θ_{tele} is the HPBW of the telescope.

The measured $v \sin i$ for Vega (15 km s^{-1}) compared to that for the ensemble of known A0V stars ($< v \sin i >= 145$ km s^{-1}) suggests an apparent inclination of the rotation axis of Vega of barely 5°. Hence, Vega may be seen straight down the rotation axis. As such, its disk should be nearly axially symmetric to the line of sight.

Assuming the circumVega disk is axially symmetric along our line of sight (*i.e.* $\Theta_{major} = \Theta_{minor} = \Theta_{vega}$), and taking $F_{total} = 17.0 \pm 5.5$ mJy, $F_{beam,IRAM} = 4.5$ mJy, and $\Theta_{IRAM} = 12''$, we can use Eqn(4) to estimate a lower limit to the source scale, Θ_{vega}. We obtain $\Theta_{vega} = 20.0^{+4.0}_{-5.0}$ arcsec. Since $\Theta_{vega} > \Theta_{IRAM}$, it is clear that the assumption that Vega is unresolved at 1300 μm at IRAM is flawed. If the source has a central hole or is not of uniform brightness, the outer radius would be even larger.

With the result $\Theta_{vega} = 20.0^{+4.0}_{-5.0}$ arcsec, we are forced to conclude that $F_{total} > 15$ mJy since only a fraction of the total source flux from such an extended object would be detected even in the CSO beam. To obtain a more accurate solution, we need to simultaneously solve

$$F_{total} = F_{beam,CSO}\left[1+\left(\frac{\Theta_{vega}}{\Theta_{CSO}}\right)^2\right], \qquad (5a)$$

$$F_{total} = F_{beam,IRAM}\left[1+\left(\frac{\Theta_{vega}}{\Theta_{IRAM}}\right)^2\right] \qquad (5b)$$

for F_{total} and Θ_{vega}. Doing so, we obtain $F_{total} = 36.1^{+48.7}_{-18.5}$ mJy and $\Theta_{vega} = 31.8^{+18.9}_{-11.3}$ arcsec at 1300 μm. Recall that IRAS found the FWHM of the circumVega source is 29″ at 60 μm. We have now shown Θ_{vega} may be comparable in size at 60 and 1300 μm and, by inference, at all wavebands between 60 and 1300 μm. Therefore, Vega should appear extended relative to the 9″ IRAM beam used at 870 μm and even to the 16.5″ beam used at JCMT at 800 μm. We conclude from our analysis of the 1300 μm data that the thermal continuum observations of Vega made at far-infrared, submillimeter and millimeter wavelengths are consistent with a picture in which the FWHM of the Vega continuum source is greater than 200 AU.

All of the observations used in this analysis are fairly low signal-to-noise results; therefore, our result is neither unique nor definitive. Nevertheless, this analysis points out clearly that our understanding of the circumVega disk, and perhaps of the dust structures around other Vega-type stars based on the currently available data, is far from conclusive at this time.

3.5 The Big Picture

We now consider other submillimeter measurements of the circumVega disk(summarized in Table 3). The 870 and 800 μm data and 2.4σ and 4.0σ results, respectively. For a grey, thermal, Planckian source, the flux density on the Rayleigh-Jeans tail is proportional to $\nu^{2+\beta}$, where β is defined by Eqn(1). For a blackbody, $\beta = 0$ and F_ν is proportional to ν^2. Therefore F_ν for an isothermal blackbody will be 18% greater at 800 μm than at 870 μm. For a greybody with $\beta = 1$, the difference will be 29%. Therefore, even for a point source, more flux should be detected through the 800 μm JCMT filter than in 870 μm IRAM observations of the same object. If the source is extended relative to the smaller (9″) IRAM beam, the observed difference will be even larger, since the HPBW at JCMT (16.5″) is larger. From Eqn(4) and taking $\Theta_{vega} = 19.5$, we estimate that at JCMT, one should measure $F_{beam} \leq 0.41\ F_{total}$ at 800 μm. At IRAM, $F_{beam} \leq 0.17\ F_{total}$ at 870 μm. Therefore, taking into account both the shape of the source spectrum and the relative beam sizes, we predict that a measurement of the extended source at JCMT at 800 μm would yield 2.5 times more flux than an IRAM measurement at 870 μm. Yet, there is no difference between the two published results (Chini90, ZB93). Therefore, even knowing that the 60 μm FWHM is 29″, one would conclude that the 800 and 870 μm observations can be made consistent only if the submillimeter source size is smaller than the 9″ beam used at 870 μm; however, we have previously concluded that the source size must be larger than this in order to remove the apparent discrepancy in the 1300 μm observations.

We are therefore left to conclude either that i) there is astrophysical flux in at least some of the Vega OFF beams or ii) one or more of the reported observations at 800, 870 or 1300 μm is in error. Since we have no reason to suspect that the IRAM observations are incorrect, we take a closer look at the CSO results.

We could reconcile all the data sets by concluding that the 500 AU data set taken at CSO yields a flux density that is 11 mJy (2σ) too high. The actual flux density may be fully 1σ (5.5 mJy) less than the nominal value of 17.0 mJy, but statistically it is much less likely that the true flux in this beam is as low as 6 mJy. However, if we combine the 500 AU and 1000 AU data sets from CSO we obtain 6.7 $\pm$ 3.9 mJy, a result apparently consistent with the Chini90 observations. To obtain this result, we retain 798 out of 800 data points. These are all of those within 3.5σ of the mean, tossing out, only two points 5.4σ and 7.3σ from the mean. Is this reasonable? A careful examination of the six 500 AU chop observations of Vega (Table 2a) reveals that the absolute signal level varied but was always positive. Inspection of the five 1000 AU chop

observations of Vega reveals that the signal strength is positive in two observation sets and negative in three sets. The weather observations for these two data sets were identically dry and stable yet the statistical means for these two data sets (17.0 and −2.6 mJy) differ by more than 3σ. One might conclude that the 1000 AU chop (123″) was too large, yielding poor atmospheric cancellation. This might explain the positive to negative variations in those five observations. If we accept this explanation, however, we would ignore these five observations, and have no justification for combining all 11 observations. If we choose to accept that the atmospheric cancellation was satisfactory in the 1000 AU chop data set, it appears hard to justify combining both data sets into one when the mean values of each differ by what appears to be a statistically significant amount. Thus, our final results remain 17.0 ± 5.5 mJy with a 500 AU chop and $\leq$ 15.9 mJy (−2.6± 5.3 mJy) with a 1000 AU chop.

Instead of assuming the CSO data set is in error, we could assume the IRAM observations are in error. The 17.0 mJy result at 1300 μm implies flux densities of at least 45 mJy ($\beta = 0$) and possibly as much as 73 mJy ($\beta = 1$) at 800 μm (38 and 57 mJy at 870 μm). Such flux densities are far above those found in the submillimeter observations of Chini90 and ZB93, even with a substantial allowance for errors. We therefore would have to assume, in addition to the IRAM 1300 μm result, that both the 870 and 800 μm observations were also in error, which seems unlikely. We either must throw out virtually all of the observations of Vega as erroneous, or we must conclude that certain observations are missing some flux.

In summary, we are forced to draw one of two conclusions in order to reconcile *all* these data sets. ***First, the FWHM of the circumVega source is likely greater than 31″ at submillimeter and millimeter wavelengths. Second, some of the OFF beams contain positive astrophysical flux.*** Alternatively, it remains possible to assume Vega is unresolved and that any or several of the observations, including our CSO data sets, or our interpretation of the CSO data sets, is incorrect. Our purpose, herein, however, is to demonstrate that a non-standard model of Vega and Vega-type stars is consistent with the extant data. We therefore continue in our analysis by asking why Chini90 measured such a low flux at 1300 μm if the source is actually as bright as the 17.0 mJy determine by us at CSO.

If the cold dust source is as much as 50″ across, Chini90 would have chopped away positive flux in the 12″ OFF beam only 30″ (240 AU) from the star. If they chopped away positive flux in the 1300 μm observations, they likely chopped away positive flux in the 870 μm observations, made with the same throw. Therefore, both these observations would give only lower limits for the flux densities along the line of sight to Vega. Since we have concluded that the ZB93 measurement is too low compared to the Chini90 result, provided the emission source is at least as extended as the IRAM beam, we similarly would conclude that ZB93 chopped away some flux in their OFF beam 40″ (320 AU). Therefore, the diameter of the extended emission source around Vega might be as large as 80″ (650 AU).

The absolute peak flux at wavelength λ (in microns), as well as the flux in the extended emission regions, can be estimated from the formula

$$F_{total,\lambda} = (1300/\lambda)^{2+\beta} F_{beam,1300}\left[1 + \left(\frac{\Theta_{vega}}{\Theta_{CSO}}\right)^2\right], \quad (6)$$

using the 1300 μm source size calculated from Eqn(5), $\Theta_{vega} = 31.8''$, and the observed 1300 μm F_{beam} for Vega, 17.0 mJy. At a minimum ($\beta = 0$), the 800 μm total flux will be 95 mJy. Based on this source size and the JCMT beam size considerations, we already showed that $F_{beam,JCMT} \sim 0.4\ F_{total}$ at this wavelength. Therefore, we estimate $F_{beam} \sim 37$ mJy at 800 μm. Since ZB93 measured 21.5 ± 5.4 mJy, the 800 μm flux 40″ from Vega (their OFF positions) may be as much as 15 mJy.

We now reexamine the CSO observations from the perspective that the circumVega disk is extended. When we used a 62″ chop (500 AU), we measured 17.0 ± 5.5 mJy. When we chopped twice as far, we obtained a result consistent with zero net flux, -2.6 ± 5.3 mJy (≤ 15.9 mJy). Yet, we know that the 1300 μm peak flux density is most likely in the range of 11.5 to 22.5 mJy. Therefore, the 1000 AU chop may have subtracted as much as 22 mJy in the OFF beam. If the flux in the OFF beams tends toward the upper end of these ranges, a radial profile of the flux from the environment of Vega would reveal 15 to 20 mJy within a radius of one-half beam width (120 AU) of the star, less than 5 mJy in the region centered 500±120 AU from the star, and as much as or more than 20 mJy in the region centered 1000±120 AU from the star (Fig. 2). These results suggest that the circumVega disk could be 1000 AU in radius with a thinned region, such as a toroidal gap, in the vicinity of 500 AU radius.

Intriguingly, this is what one predicts for the radial profile of dust in our Kuiper Disk and Oort Cloud (Stern *et al.* 1991). It is also interesting to note that Vega has a secondary, α Lyr B ($\Delta m = 10.4$; ([V] = 10.43), located 62.8″ (510 AU) distant.

The peak 1300 μm flux of ~17 mJy corresponds to $0.002\ M_\oplus < M_{dust} < 0.07\ M_\oplus$ within ~120 AU of Vega (see Eqn(3)). A similar amount of mass within a single 30″ OFF beam, located 123″ from the star, is implied by our non-standard interpretation the 1000 AU chop results. Since Vega is seen nearly pole-on, the circumVega disk should display plane-of-the-sky symmetry. Thus, the single OFF beam may represent as little as 4% of the surface area of the disk located within one beam of $r = 123''$. Therefore, the total dust mass in the regions of the Vega disk near 1000 AU may be as much as 0.05 $M_\oplus$ (for $\beta = 0$) or 1.5 $M_\oplus$ (for $\beta = 2$). $M_\oplus$. The annulus centered at 500 AU may contain much less dust (and mass per beam area) than that seen either toward the star or in the $r = 1000$ AU region.

For dust grains around Vega, Backman and Paresce (1993) show that inside of ~ 40 AU, grains are destroyed by collisions on a time scale comparable to that of Poynting-Robertson (P-R) drag. Beyond ~ 40

AU, however, the dominant loss process is P-R, which limits low-eccentricity grain lifetimes to

$$\tau_{PR} \approx 7.1 \times 10^2 \; a_{\mu m} \; \rho \; R_{AU}^2 \; L_*^{-1} \text{ yr.} \tag{7}$$

Here R_{AU} is the grain's astrocentric semi-major axis in AU, a is the grain radius in microns, ρ is the grain density in g cm^{-3}, and L_* is the stellar luminosity in $L_\odot$ (Burns *et al.* 1979; Backman and Paresce 1993). Even as far as 1000 AU from Vega, the P-R lifetime would be only 1.2×10^7 yr for a particle with unit density and 1 cm radius. How does this compare with the age of Vega? From the revised Yale isochrones (Green *et al.* 1987), Backman and Paresce estimate that the age of Vega is $4 \pm 1.2 \times 10^8$. They also point out that Vega is significantly brighter than its ZAMS luminosity and that the isochronal age is near the end of the predicted main-sequence lifetime for an A0 star. Thus, at 1000 AU, τ_{PR} is ~ 30 times shorter than the 4×10^8age of Vega. At 100 AU, τ_{PR} decreases to only $\sim 10^5$ yr. The actual residence times for dust grains are likely to be even shorter, of course, since grain-grain collisions in the disk and ISM drag will also act to clear out small particles (Lissauer and Griffith 1989; Stern 1990). Although large grains ($a > 30$ μm) might survive at 1000 AU for the lifetime of Vega, at 100 AU grains as large as 1 mm would have lifetimes much less than that of Vega. Thus, submillimeter and millimeter observations therefore provide strong evidence for recent dust production around Vega.

4. ANALYSIS OF PHOTOMETRY OF OTHER MAIN-SEQUENCE IR EXCESS SOURCES

4.1 Fomalhaut

The 1300 μm map of Fomalhaut, reported by Stern *et al.* 1994 (hereafter SFW94), appears to reveal an emission source at least 190 AU (east-west) by 150 AU (north-south) in extent. This and other previously reported millimeter and submillimeter observations of this IRAS IR excess star (Chini90; Chini91; ZB93; and Mannings & Emerson 1993) are presented in Table 3. As suggested above for Vega, it is possible that some chopping observations of Fomalhaut underestimate the true source flux because the source region is larger than the chop scales.

We made 1300 μm, single-element bolometer observations of Fomalhaut at CSO during the same run as our observations of Vega (Table 2a). The complete set of these new 1300 μm observations reveal a marginal result ($+7.7 \pm 12.0$ mJy; or $\leq$36.0 mJy). This upper limit is consistent with all previously reported results; thus our new data do not provide additional constraints on interpreting the extant Fomalhaut data. Thus, we now examine the other published data for Fomalhaut and consider in more detail whether the complete body of data is internally consistent.

As a starting point, we assume the chop positions used in the 1300 μm observations of Fomalhaut by Chini90 and Chini91 were empty of astrophysical flux. The observations from IRAM (Chini90; Θ_{IRAM} =

12″) and SEST (Chini91; $\Theta_{SEST} = 24''$) reveal three times more flux in the larger SEST beam (Table 3). The 13.7 mJy difference between these measurements is far greater (more than 5σ) than the reported errors (2.2 and 2.5 mJy). These results are self-consistent *only* if the emission source around Fomalhaut is extended (or if one of the observations is wrong). Assuming 21 mJy, as measured at SEST, is the total flux density and 7.3 mJy, as measured at IRAM, is the flux density per beam in the IRAM data, we find from Eqn(4) that the FWHM of the long wavelength emission source around Fomalhaut (Θ_{fom}) must be at least 22″. However, if $\Theta_{fom} = 22''$, Eqn(4) also indicates that only 50% of the total flux should be in the SEST beam. Therefore, as before, we must solve simultaneously for the source size and the total flux,

$$F_{total} = F_{beam,SEST} \left[1 + \left(\frac{\Theta_{fom}}{\Theta_{SEST}}\right)^2\right], \tag{8a}$$

$$F_{total} = F_{beam,IRAM} \left[1 + \left(\frac{\Theta_{fom}}{\Theta_{IRAM}}\right)^2\right]. \tag{8b}$$

Using the IRAM and SEST data, we find $\Theta_{fom} \geq 31''$ and $F_{total} \geq 56$ mJy. Notably, this result for Θ_{fom} is consistent with the measurement of a FWHM of 45″ in 100 μm emission by Lester *et al.* (1989). ZB93 also conclude, from 800 μm data, that the source scale at 800 μm is about the same as that determined at 100 μm.

We note here that Chini90 (for 870 μm observations) and ZB93 (for 800 μm observations) used chop throws of only 30″ and 40″ with HPBWs of 12″ and 16.5″, respectively. For a source with $\Theta = 31''$, these throws and beam sizes barely reach beyond the FWHM of the extended source. If $\Theta_{fom} > 31''$, both of these observations would have chopped onto the extended source. To illustrate this, let $\Theta_{fom} = 40''$. Then one would still obtain the IRAM and SEST beam fluxes if $F_{total} = 80$ mJy. Therefore, one would expect to have chopped away some additional flux in the IRAM and JCMT OFF positions. We would thus conclude that $F_{total} > 80$ mJy. Although the extended source might emit more than 80 mJy, the flux per beam area would always be small and our ability to measure the true flux in chopping observations would be diminished because of the extended nature of the source.

The self consistent solution we have found for the 1300 μm IRAM and SEST observations leads to a prediction that one would find 27 mJy in the CSO 30″ beam, which is consistent with our upper limit. The presence of flux in the OFF positions also could explain the complete set of Fomalhaut observations.

At 870 and 800 μm, Chini90 (35 $\pm$ 12 mJy) and ZB93 (35 $\pm$ 6.5 mJy) obtained nearly identical flux densities along the line of sight toward Fomalhaut. As discussed before, a minimum of 18%-29% more flux (depending on β) should be detected at 800 μm than at 870 μm. For an extended source, more flux should be detected in the larger JCMT beam than in the smaller IRAM beam. Such differences are not demonstrated by the data, although they are within the limits of the errors of these measurements. If we extrapolate the

SEST observations to shorter wavelengths, assuming Fomalhaut is an unresolved source, we would predict at least 47 ± 6 mJy of flux at 870 μm (for $\beta = 0$) and 55 ± 7 mJy at 800 μm. Thus, neither submillimeter result is consistent with the 1300 μm SEST observation if Fomalhaut is an unresolved source. The absence of significant differences between the 800 and 870 μm results could be explained by an error in one of the data sets. Alternatively, if Fomalhaut is extended there could be additional flux in the OFF beam positions and both observations could be correct.

We cannot establish the absolute Fomalhaut flux levels at millimeter wavelengths from this analysis. It is clear, however, that *the complete set of observations of Fomalhaut demand that either a) the source is extended relative to the HPBWs of all the telescopes used, or b) several of the published observations are in error, or both.*

4.2 ϵ Eri and τ^1 Eri

ϵ Eri and τ^1 Eri are IRAS IR excess stars observed by Chini90, Chini91 and ZB93 (Table 3). We now use all of these millimeter and submillimeter data sets to form a self-consistent picture of these sources. Under the assumptions that only a single population of warm dust grains surround these stars and that the 100 μm emission is on or nearly on the Rayleigh-Jeans tail, we can estimate the 1300 μm flux densities from these dust disks using their 100 μm excesses (2.27 Jy for ϵ Eri; 3.65 Jy for τ^1 Eri; Backman and Paresce 1993). The expected emission from the ϵ Eri dust disk should be between 0.08 mJy ($\beta = 2$) and 13 mJy ($\beta = 0$). Toward τ^1 Eri we predict 0.1 mJy ($\beta = 0$) to 22 mJy ($\beta = 2$). If additional cold dust is present that went undetected by IRAS, or if the Rayleigh-Jeans assumption is incorrect, the 1300 μm flux densities could be greater still. In fact, Chini91 measured ~20-25 mJy toward both stars at 1300 μm at SEST but much smaller flux densities in the smaller IRAM beam. Chini91 pointed out that for these stars, as for Fomalhaut, the IRAM and SEST data are consistent with an increase in emission at 1300 μm that is directly proportional to beam area. Chini91 suggested that both stars are surrounded by dust free cavities (of diameters 4.2″ and 7.7″, respectively) and dusty annuli (outer diameters 22″ and 17.5″, respectively). Whether or not the Chini91 model applies, the data leave no doubt that the 1300 μm emission sources around both stars are extended. Consequently, the sources are resolved and the data from IRAM and JCMT should be treated as measurements of F_{beam}, rather than F_{total}.

We can extrapolate from the 1300 μm results to predict the flux densities F_λ of these stars at shorter wavelengths. We assume the flux density is proportional to $\nu^{2+\beta}$ with $2 \geq \beta \geq 0$. For ϵ Eri, the IRAM result (7.5 mJy) implies 37 mJy $\geq F_{870} \geq$ 17 mJy in the IRAM beam and 52 mJy $\geq F_{800} \geq$ 20 mJy in the JCMT beam. The short wavelength fluxes would be more than three times greater if we extrapolate from the SEST data (24.2 mJy). The Chini90 result (35 ± 13 mJy at 870 μm) is consistent with these predictions. The

ZB93 observation (7.7 ± 7.7 mJy at 800 μm), however, is only marginally consistent with the IRAM based extrapolation, and only so if we treat it as a 3σ upper limit of 23 mJy. Since the beam used by ZB93 was larger than the IRAM beam but smaller than the SEST beam, they should have detected more flux at 800 μm than Chini90 detected at 870 μm.

Similarly, we extrapolate the Chini90 observation of τ^1 Eri to shorter wavelengths. From the IRAM result (< 6.6 mJy), we predict an upper limit of 15 mJy ($\beta = 0$) to 30 mJy ($\beta = 2$) at 870 μm and upper limits of 17 mJy and 46 mJy at 800 μm. Chini90's and ZB93's reported flux density measurements at 870 μm and 800 μm are consistent with these upper limits. However, Chini91 detected a fairly strong signal of 20.7 mJy from τ^1 Eri at 1300 μm. If all the data for this star are to be reconciled, and assuming no flux is removed in the OFF beams, most of the 1300 μm flux must come from outside the JCMT beam.

In the case of ϵ Eri, the large amount of flux detected by Chini91 compared to that detected by Chini90 and ZB93 may simply be due to the larger chop used in the SEST measurements. In this interpretation, the disk may extend as far as 30″-40″ from the star but would not extend as far as 70″. For τ^1 Eri, the measurements can be satisfactorily interpreted in the same way; in this case however, the disk must be more than 500 AU in radius.

5. SUMMARY

We have shown that significant discrepancies appear to exist in the literature for millimeter and submillimeter continuum observations of four main-sequence IRAS IR excess stars (Vega, Fomalhaut, ϵ Eri and τ^1 Eri). Furthermore, we have shown that most, if not all, of the discrepancies can be removed by assuming that the sources are of order hundreds of AU in extent (Table 4).

Single-element bolometers and the ON-minus-OFF chopping technique were employed for most of the reported submillimeter and millimeter observations of IRAS IR excess stars. For sources that may be extended or are of unknown geometry, this observing technique only provides relative measurements, specifically only lower limits to the true flux densities of the sources, and must be applied with caution.

In the cases of Vega and Fomalhaut, and perhaps ϵ Eri, τ^1 Eri and many more IRAS IR excess stars, it is reasonable to argue with the existing data that the OFF positions may not be empty. Instead, the OFF positions may include detectable levels of flux from cold dust grains at large circumstellar distances. As such, disk mass calculations based on these observations should be reexamined. Given the physically limited chop throws of submillimeter/millimeter telescopes, it appears that mapping, rather than simple ON-minus-OFF observations, are required to elucidate the true nature of the dusty structures surrounding nearby, IRAS IR excess sources.

SAS acknowledges NASA's Origins of Solar Systems Program for support. We also thank the CSO staff for support. The CSO is operated by Caltech with support from the NSF under grant AST 9015755.

REFERENCES

Allen, C.W. 1973, Astrophysical Quantities (London: The Athlone Press)

Altenhoff, W.J., Chini, R., Hein, H., Kreysa, E., Mezger, P.G., Salter, C., & Schraml, J.B. A&A, 190, L15 (1988)

Aumann, H.H., Gillett, F.C., Beichmann, C.A., de Jong, T., Houck, J.R., Low, F.J., Neugebauer, G., Walker, R.G., & Wesselius, P.R. 1984, ApJ, 278, L23-27

Backman, D.E., & Paresce, F. 1993, In *Protostars and Planets III* (Eds. Levy, E., Lunine, J.I., Matthews, M.S.), (Univ. of Az. Press, Tucson, Az) 1253-1295

Burns, J., Lamy, P.L., & Soter, S. 1979, Icarus, 40, 1

Chini, R., Kreysa, E., & Gemund, H.-P. 1984, A&A, 137, 117

Chini, R., Krügel, E., & Kreysa, E. 1990, A&A, 227, L5-11

Chini, R., Krügel, E., Shustov, B., Tutukov, A., & Kreysa, E. 1991, A&A, 252, 220-228

Gillett, F. 1986, in *Light on Dark Matter*, Ap. Space Sci. Library 124, ed. F.P. Israel (Dordrecht: D. Reidel Co.), p. 61

Green, E.M., Demarque, P., & King, C.R. 1987, *The Revised Yale Isochrones and Luminosity Functions*, (Yale Univ. Obs., New Haven)

Griffin, M.J. *et al.*, 1986, Icarus, 65, 244-258

Hildebrand, R.H. 1983, QJRAS, 24, 267-282

Lissauer, J.J., & Griffith, C.A. 1989, ApJ, 340, 468

Mannings, V., & Emerson, J.P. 1993, IAU Circular 5786

Orton, G.S. *et al.*, 1986, Icarus, 67, 289-301

Sandell, G., & Weintraub, D.A. 1994, A&A, submitted

Stern, S.A. 1990, Icarus, 84, 447-466

Stern, S.A., Stocke, J., & Weissman, P.R. 1991, Icarus, 91, 65-75

Stern, S.A., Festou, M.C., & Weintraub, D.A. 1994 Nature, submitted

Stern, S.A., Weintraub, D.A. and Festou, M.C. 1993, Science, 261, 1731

Zuckerman, B. and Becklin, E.E. 1993 ApJ, 414, 793

TABLE 1: Stellar Characteristics

Star	Other Names	Spectral Type	Distance (pc)	Luminosity[a] ($L_\odot$)	Mass[a] ($M_\odot$)
α Lyrae	HR 7001, Vega	A0Va	8.1	60	2.5
α PsA	HR 8728, Fomalhaut	A3V	6.7	13	2.0
ϵ Eri	HR 1084	K2V	3.3	0.3	0.75
τ^1 Eri	HR 818	F6V	13.7	2.2	1.2
β Leo	HR 4534	A3V	12.1	25	2.2

a — Luminosities and Masses for α Lyrae and α PsA from Backman & Paresce (1993); values for other stars estimated from Allen (1973).

TABLE 2a: New 1300 μm Continuum Observations from CSO

Time & Date (1993 UT)	Air-mass[a]	Zenith Optical Depth[a]	Chop Distance (AU)	Chop PA (deg)	Number 9 s Cycles Collected	Number 9 s Cycles Used[b]	Flux Density (mJy)	S/N
				Vega				
14:04 April 15	1.106	0.069	500	40.9	40	40	$+46.8 \pm 20.4$	+2.3
14:19 April 15	1.088	0.070	500	33.2	40	39	$+6.3 \pm 17.0$	+0.4
14:43 April 15	1.069	0.067	500	18.4	40	40	$+39.7 \pm 17.9$	+2.2
14:57 April 15	1.061	0.067	500	8.1	40	40	$+2.4 \pm 18.6$	+0.1
13:57 April 16	1.110	0.046	500	31.0	100	99	$+16.7 \pm 9.0$	+1.9
14:44 April 16	1.066	0.043	500	−0.9	100	100	$+5.7 \pm 9.3$	+0.6
11:45 April 15	1.561	0.066	1000	77.1	100	100	$+16.1 \pm 12.8$	+1.3
12:33 April 15	1.324	0.067	1000	65.9	100	100	-10.0 ± 10.5	−0.9
13:21 April 15	1.181	0.068	1000	58.2	40	40	$+2.7 \pm 20.2$	+0.1
12:15 April 16	1.381	0.043	1000	69.5	100	100	-11.3 ± 11.4	−1.0
13:03 April 16	1.217	0.043	1000	55.2	100	99	-6.6 ± 9.2	−0.7
				Fomalhaut				
15:33 April 15	3.863	0.064	1000	−52.7	100	100	-7.7 ± 27.2	−0.3
16:12 April 15	2.980	0.062	1000	−49.3	50	50	$+24.8 \pm 22.0$	+1.1
15:37 April 16	4.212	0.039	1000	−51.3	100	100	$+9.1 \pm 12.1$	+0.8
				β Leo				
8:22 April 15	1.006	0.072	1000	45.4	100	100	$+5.4 \pm 9.2$	+0.6
9:01 April 15	1.009	0.069	1000	68.0	100	100	-1.9 ± 11.4	−0.2

a — Average from beginning to end of observation.

b — After removing obvious cosmic ray contaminated data points.

TABLE 2b: Net Results: 1300 μm Continuum Observations from CSO

Star	Chop Distance	Number 9 sec Cycles	Integration Time (sec)	Flux Density[a] (mJy)	S/N[b]
Vega	500	358	3,222	$+17.0 \pm 5.5$	+3.1
Vega	1000	439	3,951	≤ 15.9	−0.5
Fomalhaut	1000	249	2,241	≤ 36.0	+0.6
β Leo	1000	200	1,800	≤ 21.3	+0.3

a — or 3σ upper limit.

b — where noise is taken as the 1σ level.

TABLE 3: Summary of Direct Line-of-Sight CSO Photometry of Vega-like Stars

Observer	Wavelength (μm)	HPBW (arcsec)	Telescope	Chop (arcsec)	Chop (AU)	Flux Density (mJy)
			Vega			
Chini90	1300	12	IRAM	30	240	4.5 ± 1.5
This Work	1300	30	CSO	62	500	17.0 ± 5.5
This Work	1300	30	CSO	123	1000	≤ 15.9
Chini90	870	9	IRAM	30	240	22 ± 9
ZB93	800	16.5	JCMT	40	320	21.5 ± 5.4
			Fomalhaut			
Chini90	1300	12	IRAM	30	200	7.3 ± 2.2
Chini91	1300	24	SEST	70	470	21 ± 2.5
Mannings & Emerson 1993	1300	19.8	JCMT	90	600	1 ± 8
This Work	1300	30	CSO	150	1000	<36.0
SFW94	1300	12	IRAM	Map[1]	Map	32 ± 12
Chini90	870	9	IRAM	30	200	35 ± 12
ZB93	800	16.5	JCMT	40	270	35 ± 6.5
			ϵ Eri			
Chini90	1300	12	IRAM	30	100	7.5 ± 2.2
Chini91	1300	24	SEST	70	230	24.2 ± 3.4
Chini90	870	9	IRAM	30	100	35 ± 13
ZB93	800	16.5	JCMT	40	130	7.7 ± 7.7
			τ^1 Eri			
Chini90	1300	12	IRAM	30	410	<6.6
Chini91	1300	24	SEST	70	960	20.7 ± 3.9
Chini90	870	9	IRAM	30	410	<30
ZB93	800	16.5	JCMT	40	550	-7.7 ± 7.3
			β Leo			
This Work	1300	30	CSO	83	1000	<21.3

1 — For map, flux density is that in the central beam.

TABLE 4: Summary: Disk Masses and Radii from 1300 μm Continuum Observations

Star	Dust Mass Along Line-of-Sight to Star ($M_\oplus$)[a]	Radius (AU)
Vega	0.002 - 0.07	$\leq$1000
Fomalhaut	$< 0.003 - < 0.08$	$\leq$ 600
β Leo	$< 0.007 - < 0.2$	...
ϵ Eri	0.0006 - 0.02	$\leq$ 130
τ^1 Eri	0.009 - 0.2	$\leq$ 500

a — range corresponds to $\beta = 0$ (minimum) and 2 (maximum).

FIGURE CAPTIONS

FIG. 1. Bolometer chopping data is collected in a two-part cycle in which the telescope points alternately at the position of the star and a position offset from the star by a specified distance. The offset position is presumed to be empty of astrophysical sources. In order to compensate for gradients in the local sky emission, the telescope collects "sky" data in the second half of the cycle in the opposite direction on the sky from that selected in the first half of the cycle.

FIG. 2. The CSO observations of Vega are illustrated by the bar graphs. Our measurements yield 15.1 $\pm$ 5.4 mJy with a 500 AU chop. These results indicate that 15 mJy more flux is emitted from the vicinity of the star than in a beam placed 500 AU from the star. Measurements with a 1000 AU chop are consistent with zero flux, indicating that a beam placed 1000 AU from the star yields a comparable amount of flux as a beam placed on the stellar position. Our preferred interpretation of these results is illustrated in the overlay: a (comparatively) empty annulus (of unknown width) located 500 AU from Vega truncates a circumstellar dust disk that extends at least as far as 1000 AU from the star.

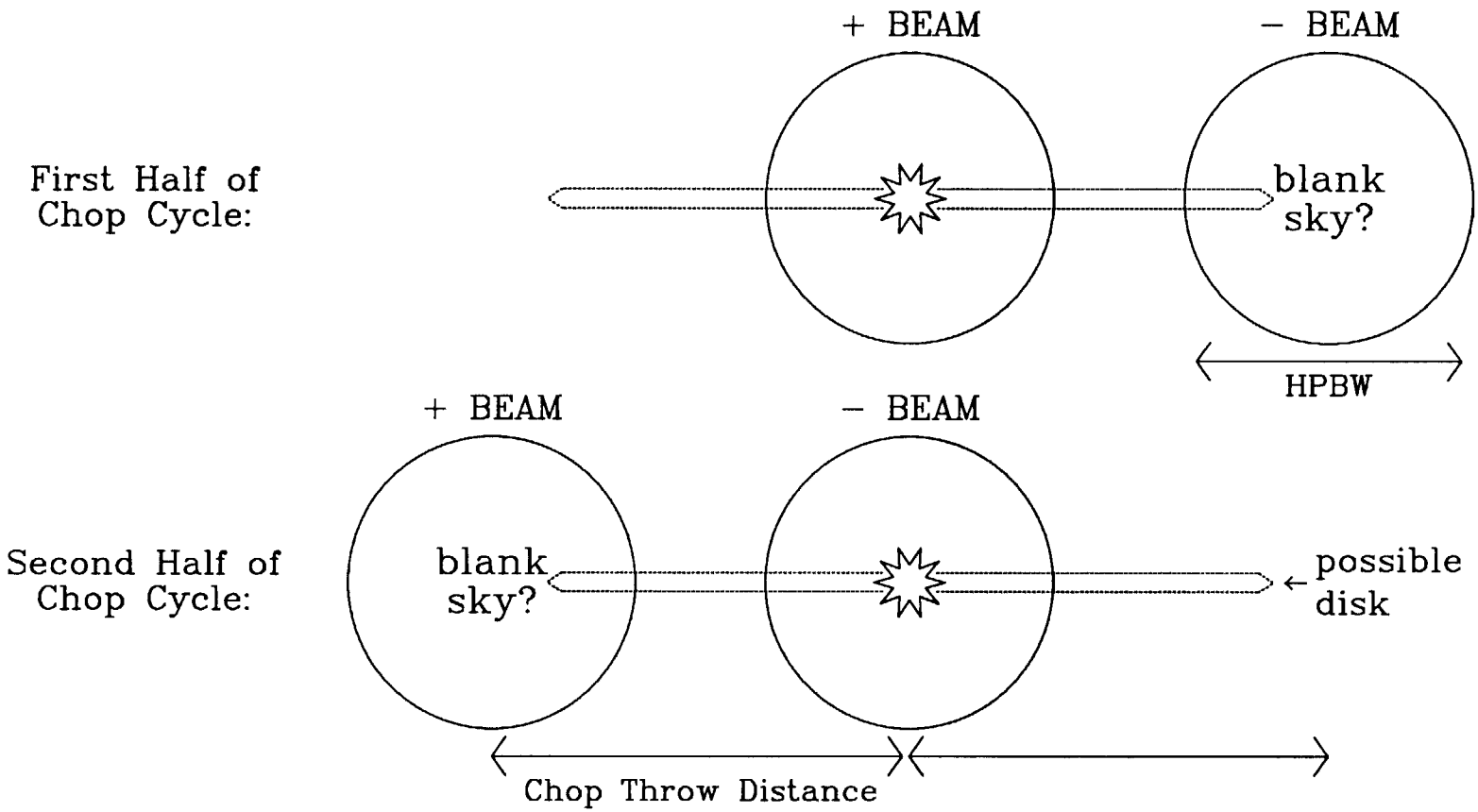
+ BEAM
− BEAM
First Half of
Chop Cycle:
blank
sky?
HPBW
+ BEAM
− BEAM
Second Half of
Chop Cycle:
blank
sky?
possible
disk
Chop Throw Distance

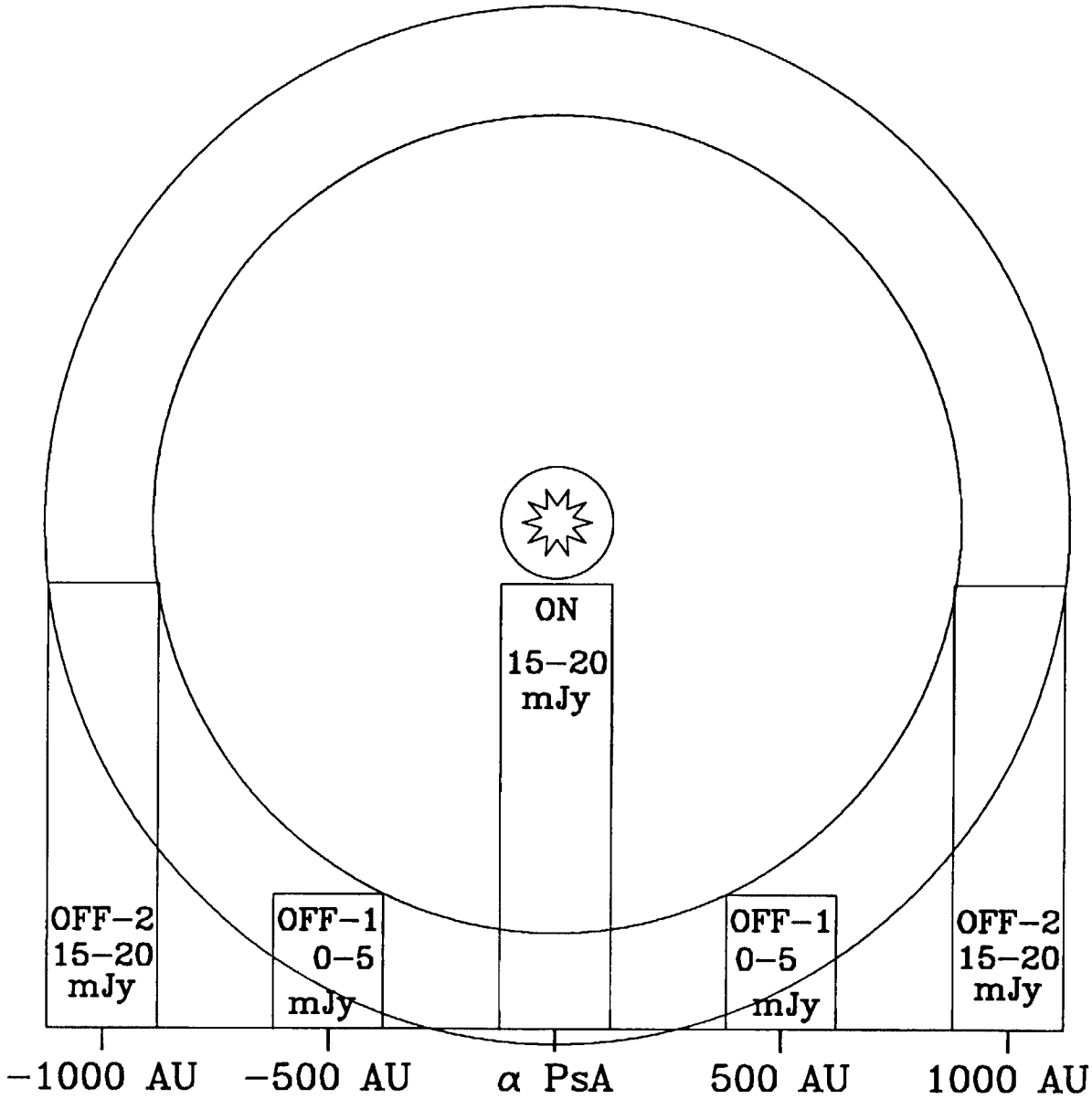
ON
15–20
mJy
OFF–2
15–20
mJy
OFF–1
0–5
mJy
OFF–1
0–5
mJy
OFF–2
15–20
mJy
−1000 AU
−500 AU
α PsA
500 AU
1000 AU

APPENDIX C

Chiron: Interloper from the Kuiper Disk?

(Stern, 1993)

Chiron: Interloper from the Kuiper Disk?

An Article for Astronomy Magazine

S. Alan Stern[1]
[210]522-5127 (voice)
[210]647-4325 (fax)

12 December 1993

[1]Alan Stern is a planetary scientist at the Southwest Research Institute in San Antonio.

A Stranger in a Strange Land

It struck many astronomers as strange and intriguing when, in 1977, Charlie Kowal of the Hale Observatories discovered Chiron. Although Chiron was officially labeled asteroid number 2060 by the Minor Planet Center, this designation always seemed a little uncomfortable. After all– what was an asteroid doing on a 51-year orbit that crossed inside the orbit of Saturn and then travelled outward almost to Uranus? Could Chiron be a comet?

Probably not, at least by conventional standards. Based on its brightness (then V$\approx$19) and distance from the Sun (then 17 AU), it was possible to estimate Chiron's size. Chiron was monsterous compared to any typical comet. Based on the similarity of its surface spectrum to C-type asteroids, Bill Hartmann of the Planetary Science Institute in Tucson estimated Chiron's surface albedo (i.e., its reflectance) was near 10% and its diameter was between 130 and 400 km. About the same time, University of Arizona astronomer Larry Lebofsky and colleagues made the first thermal detections of Chiron, and used these data to derive a diameter near 180 km. Later measurements by other groups using spacecraft and groundbased facilities to search for or detect Chiron's thermal emission now indicate Chiron is most likely between 200 and 350 km in diameter. Compare that to the 3-10 km diameters of common comets and you find Chiron to be a distant outlier, an Empire State Building among garden homes.

Clearly, Chiron didn't seem to fit into any of the existing categories: too small to be a planet, too distant to be a conventional asteroid, and too large to be a conventional comet. What made the situation more difficult was that Kowal had detected Chiron as a part of a deep survey that reached magnitude 20 in a wide area centered on the ecliptic. For all his careful work, Kowal found *only* one significant object, Chiron, in all the outer solar system. Perhaps 2060 Chiron was just an odd bird, moving slowly across Aries. Life went on.

The '70s came and went. So did the early and mid-1980s, and still Chiron remained a lonesome dove, a curiosity, an enigma. In the first decade after its discovery, only a few facts were learned about Chiron. For example, it was found that Chiron's present orbit is unstable and probably short lived. Also, it was learned that Chiron rotates in 5.92 hours, and displays a lightcurve amplitude of 9%. This indicates the object is either subtly spotted, or is not quite round, or both. These facts were useful, but still not very revealing of Chiron's true nature. Fortunately, beginning just after the 10th anniversary of its discovery, more interesting discoveries began to break loose.

The best break came when Dave Tholen of the University of Hawaii detected a sudden brightening of Chiron in early 1988. With colleagues Bill Hartmann, Karen Meech, and Dale Cruikshank, Tholen quickly confirmed a near-doubling in Chiron's brightness, from a V magnitude of about 18 to 17.2. But, at 13 AU, what

could cause this to happen? Had Chiron been struck by a boulder, causing some bright material to be splashed up on its surface? Had a geyser gone off, coating the surface with bright material? Had a coma formed? What was it? The chase was on. Unfortunately, Chiron wasn't yielding its secrets very easily.

Often times, when you can't say what *is* going on, you can rule out some things that *are not*. That tried and true trick in mind, in 1988 I undertook a project that asked, "Was it possible Chiron's surface could be active in the same way as a comet, surface ices to form a tenuous coma?" To answer this question, it was necessary to construct a computer model that estimated first the temperature of Chiron's surface, and then the temperature-dependent sublimation rates of various ices that had been detected across the solar system. Since the surface temperature is cooled by subliming ices, and the rate of ice sublimation depends on the surface temperature, the model involved the simultaneous solution of a pair of equations. What I found was twofold. First, ordinary water-ice (H_2O), which fuels the production of a coma in most comets won't do at Chiron– Chiron's orbit simply lies too far from the Sun to be warm enough for water ice to sublimate. Instead, something much more volatile, and more exotic, like carbon dioxide (CO_2), carbon monoxide (CO), methane (CH_4), or nitrogen (N_2) ice was required. Second, and even more interestingly, it turned out that if Chiron had spent any significant fraction of the age of the solar system in an orbit closer to the Sun than it was now, it would have sublimated away so much ice that it would not be active today. Apparently, either Chiron was a recent entrant from a *more distant* region of the solar system, or the cause of Chiron's brightening was not related to surface ice sublimation at all. More clues to narrow down the options were found soon thereafter.

The first new clue came in 1989 when Karen Meech of the University of Hawaii in Honolulu and Mike Belton of the National Optical Astronomical Observatories (NOAO) in Tucson succeeded in detecting a tenuous coma surrounding Chiron. The presence of this coma, which has at times now been seen to stretch more than 200,000 miles in diameter, clearly established that some mechanism, most likely sublimation, ejects ice and dust particles from Chiron's surface. Then, in early 1990, a team consisting of Bobby Bus and Ted Bowell of Lowell Observatory in Flagstaff, Arizona and Mike A'Hearn of the University of Maryland detected the presence of cyanogen gas (CN) in Chiron's coma. Although CN is only a trace species in cometary atmospheres, it is easier to detect than more common coma species because it fluoresces so efficiently in sunlight.

Since 1990, continued monitoring of Chiron's brightness has also revealed that Chiron's brightness fluctuates up and down, sometimes over weeks or months, by 30 to 50%. Presumably, this is because the amount of material in the coma is variable. Detailed photometric studies by Dave Jewitt and Jane Luu at the University of Hawaii, Bonnie Buratti and Scott Dunbar of JPL, and Robert Marcialis of the

University of Arizona have even detected seemingly random night-to-night and hour-to-hour fluctuations in the coma brightness of a few percent. Most interestingly, a team of astronomers led by Bobby Bus (now at MIT) reanalyzed old images of Chiron, taken before its discovery. When these images were made between 1969 and 1972, Chiron was not even known to be on the plates! After careful examination of these images, however, Bus and co-workers found that Chiron was brighter then, than it has been since. This was surprising because Chiron was near its aphelion at 19.5 AU during that period. This indicated that whatever was driving Chiron's activity, it was capable of operating not just at 13 AU, but even in the much colder conditions at 19 AU!

Since carbon dioxide ice won't sublimate this far from the Sun, Bobby Bus and his team's data make it possible to rule CO_2 out as surface ice that caused the aphelion activity. With only carbon monoxide, methane, and nitrogen ice as remaining candidates, we seem to be closing in on an inescapable conclusion: Chiron's surface ice inventory may be more similar to Triton and Pluto than to a conventional comet.

A second implication of Chiron's sporadic activity is that the surface is probably covered by some kind of involatile mantle or crust which chokes off much of the surface from being active, and allows only episodic bursty periods, perhaps from isolated vents or fissures. This view is reinforced by calculations which show that only 0.1 to 1% of Chiron's surface has to be active in order to supply the observed coma.

Putting together everything we now know about Chiron as now, it seems to be an icy object the size of a small state (see Figure 2), travelling between the outer planets in an orbit it could not have occupied for more than a tiny fraction of the age of the solar system. Based on its activity at large distances, Chiron seems to contain exotic, low-temperature ices near its surface, perhaps with a thin veneer of silicate dust or organic materials covering most of the body. If we someday conduct a spacecraft flyby of Chiron (see the sidebar), the resulting images might show Triton-like geysers shooting hundreds of kilometers into the sky (since Chiron's gravity is so much weaker than Triton's), episodically resupplying a coma that varies in mass and brightness by large amounts as the surface vents cough and sputter.

Who Ordered That?

Why aren't there alot of Chiron's between Saturn and Uranus? Most directly, because the gravitational influences of the giant planets, Jupiter, Saturn, Uranus, and Neptune conspire to remove any object that orbits between them. In fact, detailed numerical simulations of the outer solar system by Canadian dynamicists Bret Gladman and Martin Duncan have shown that objects placed on orbits between any of the giant planets are usually gravitationally removed in no more than 1 or

2% the age of the solar system. Simulations of Chiron's specific orbit by British dynamicists Mark Bailey and Gerald Hahn made in 1990 indicate that Chiron's orbit is unstable on timescales of a few million years. This fits nicely with the view that Chiron could not still have surface ices (and therefore be active) if it had always been in an orbit as close or closer to the Sun than its present path.

Still, one wonders: where did Chiron come from and why should it, just now, be in its present, short-lived orbit? For that, we must first travel back in time 44 years.

It was a remarkable time. As the cold war was deepening and television was just being born, some of the most esteemed astronomers gathered together to write and publish a mid-century volume on where astronomy stood, and where it was going. In the 1951 volume that (titled *Astrophysics* and edited by J.A. Hynek) resulted, Gerard Kuiper wrote a prescient article on the state of solar system science. Kuiper was clearly the right person for the job: he'd just discovered the satellites Miranda and Nereid, and the atmosphere of Titan.

It's been said that Kuiper was 2/3 of the entire planetary astronomy community in the 1940s. In his chapter, Kuiper wrote about a remarkable fact– that the solar system does not peter out at its edge, but instead appears to come to a discrete boundary. That is, as Kuiper pointed out, just the planetary system apparently quits, as if there is a sharp edge near 30 AU. Kuiper asked why this is so, and concluded it was most likely because no giant planet had had the time to form beyond Neptune in the age of the solar system. Since he saw no reason why the solar nebula from which the planets were constructed should end at 30 AU, Kuiper postulated a disk or belt of leftover material, the makings of additional planets, probably lie beyond Neptune.

After *Astrophysics* was published, however, Kuiper's hypothetical structure, which is now called the Kuiper Disk or Belt, was, for decades, largely forgotten. People's ideas began to change in the early-1980s, however, when Uruguyan theorist Julio Fernandez suggested that most short period (i.e., the so-called Jupiter-family) comets might be derived from Kuiper's reservoir, if small, unseen planets imbedded in the disk were numerous enough to jar these comets loose from time to time. By the late 1980s, with fast computers at their disposal, Martin Duncan, Tom Quinn, and Scott Tremaine demonstrated that through numerical simulations that it was unlikely that the short period comets could be explained *without* a Kuiper Disk.

Why? What Duncan, Quinn, and Tremaine found was that the low orbital inclinations of the short period comet orbits could not be explained unless these comets *originated* in a flattened disk. Further work by others showed that, if this disk originally extended inward to Neptune's orbit, the gravitational perturbations by the four giant planets would work to erode the disk and bring comets into where we might detect them. Although this work involved some crucial shortcuts to make

the computations tractable, it convinced many astronomers that Kuiper's original suggestion might bear fruit: There might indeed be a debris disk beyond Neptune. Coincidentally, the stage for a new paradigm like the Kuiper Disk had been subtly set a few years before, in 1983. At that time, the Infrared Astronomical Satellite (IRAS) discovered dusty disks around a host of nearby main sequence stars like β Pic and Vega. JPL's Paul Weissman and others convincingly argued these dust disks were created by comet and/or asteroid collisions around their parent stars.

While other computational groups began debating and analyzing the results Duncan and his coworkers had obtained, it became the observers turn– the race was on to find the Kuiper Disk. And what an interesting race!

Although there were expected to be one hundred million or more comets beyond 40 AU, they are very faint– no brighter than 28th or 29th magnitude. Practically speaking, this is simply too faint to reliably make a groundbased detection today. (Although no regular-sized comet has yet been detected in the Kuiper Disk– though plans are afoot to use the repaired Hubble Space Telescope to make such a discovery.) Instead, observers hoped to find larger but rarer objects that might be much brighter– perhaps 23rd or 24th magnitude. (Remember, brighter in this context is purely relative– 24th magnitude objects are 10,000 times fainter than Pluto!) The technique most often adopted in the Kuiper Disk searches involved making deep images of the dark (new moon) sky using photographic plates or CCD arrays. The best areas to image were judged to be the opposition points, where its brightness is maximized and its apparent motion allows its distance to be easily determined.

Several groups raced to find these trees in the distant, but long-suspected forest. First they searched to 21st magnitude, then to 22nd, and then 22.5. Nothing turned up. Finally, in August 1992, Dave Jewitt and Jane Luu of the University of Hawaii discovered a slowly moving object at a magnitude of R$\sim$23.5 that turned out to lie at a distance of 44 AU! Dubbed 1992QB1, this object appears to orbit the Sun in a nearly-circular orbit that lies within a few degrees of the ecliptic. Based on a typical surface albedo of a few percent, 'QB1' is likely to be 200-250 km in diameter.

Six months later, in the spring of 1993, Jewitt and Luu discovered a second Kuiper disk object, 1993FW. And a year after QB1 was found, Luu and Jewitt found two more bodies beyond 30 AU, and a British group led by Iwan Williams found still another two, which are either in the Kuiper Disk or Neptune's trojan cloud! All six new objects have brightnesses that indicate they are between 50 and 500 km in diameter. Since all six objects have been found in a search area that totals barely two square degrees, and there are over 1000 square degrees of sky left to search, it is now predicted that between 1000 and 10,000 'QB1s' lie in the Kuiper Disk region between 35 and 45 AU. Additional objects may lie farther out.

When the discovery of the muon was announced in the late 1940s, the great

particle physicist Rabi exclaimed, "Who ordered that?" Similarly, a pre-1980s astronomer might have said the same of a burgeoning crowd of large, QB1-like bodies in the Kuiper Disk. These objects are so much larger than comets that most astronomers simply did not expect to find this kind of object in such numbers. What we appear to be detecting in the Kuiper Disk is a flock of Chirons!

Are the QB1s the tiny stillborn saplings that, as Kuiper suggested, never had the time to accumulate into another Neptune? Are they the precursors to the host of Pluto-Triton "ice dwarfs" (seperately) predicted by myself and Bill McKinnon to lie in the more distant outer solar system (see *Astronomy*, May 1992)? Are the QB1s the kinds of objects now colliding in the dusty disks around stars like β Pic, Vega, and Fomalhaut? I don't know, but I hope we will have the answers to many of these questions before the last night of 20th Century astronomy is done.

For now what is important is that astronomy has discovered what appears to be another major piece of the architecture of the Solar System: The Kuiper Disk. How massive is the disk? How far out does it stretch? Are there gaps in the disk or is it continuous? What is the size range of objects in the disk, and what are these objects made of? Are planets slowly building today beyond Neptune and Pluto? All these questions are open.

I like to make an analogy that with regard to the Kuiper Disk, we in 1994 are about where astronomy stood with the asteroid belt in 1802, when just Ceres, Juno, Pallas, and Vesta had been discovered. A whole new frontier is opening up! This time, however, there are ten-thousand QB1s (perhaps with a few even larger ice dwarfs too), and a hundred million comets, to catalog and study, as opposed to a handful of minor planets and a hundred-thousand, kilometer-class objects. We are living through a very special time!

Fences Down: Cosmic Connections

Over the past two decades, life has gotten alot more complicated for planetary astronomers. (Snide comments about the grant and review process aside)! With regard to our science, many of the tidy distinctions between object types and the architecture aspects of the solar system have become blurred.

We now know comets can become inactive and appear to be asteroids, and that some (apparent) asteroids can become active and look like comets. Since the appearance of comet Shoemaker-Levy 9 in orbit around Jupiter, we now know comets can become trapped in orbit around giant planets, temporarily become moons, and perhaps then be ripped apart by tidal forces to form gossamer-thin planetary rings. We now know there is a whole second asteroid belt in the Jovian trojan region, and yet another belt or disk of objects beyond Neptune. Faced with a compelling continuum of objects, we struggle now to distinguish the boundaries between comets and asteroids, Chirons and comets, and planets and ice dwarfs.

Coming full circle since Chiron's discovery in 1977, Chiron appears to have been well-named, for it is officially a Centaur, a beast which was neither a man nor an animal, but something in between. We also see that Chiron is not the unique, giant comet or rogue asteroid it was perceived to be in 1977, but instead merely a fortuitously close forerunner of the flock of thousands of distant, similar objects in the Kuiper Disk. Finally, we also see that the Sun, like other stars, appears to be circled by a debris disk of planetesimals, remnants from the era of planetary formation, forever orbiting in the cold vacuum beyond the distant, fully-formed planets.

Figure Captions

Figure 1: Chiron's elliptical orbit among the major planets.

Figure 2: Chiron's approximate size compared to comet Halley and the state of New Hampshire.

Figure 3: Chiron's large-scale activity since aphelion in 1970 to its present position near periehlion. Chiron's activity is represented in terms of its absolute magnitude as a function of time as it moved from aphelion at 19.5 AU in 1970 toward is upcoming 1996 periehlion at 8.5 AU. The absolute magnitude of a planetary object is computed assuming the object were always 1 AU from both the Sun and the Earth; as such, it measures the intrinsic changes in brightness due to changing surface activity or other causes.

Figure 4: A conceptual schematic of the Sun's Kuiper Disk and Oort Cloud. The Kuiper Disk, which begin around 38 AU from the Sun and may stretch beyond 100 AU, is the reservoir from which the low-inclination, short period (P$<$ 200 year) comets come. In contrast, the Oort Cloud, which stretches from 2000 to beyond 20,000 AU, is the home of both the short period high-inclination and the long period (P$>$200 year) comets.

Figure 5: Diagram showing the known objects in the deep outer solar system as a function of their distance from the Sun and their mass. Chiron is not alone.

SIDEBAR: A MISSION TO CHIRON

Chiron is presently nearing perihelion and yet is still no brighter than 16th magnitude. Even though it is almost as close to Earth as it will ever get in our lifetimes, its diameter is less than a 1/20 of an arcsec! Simply put, given these circumstances, it is almost impossible to do more than characterize Chiron's bulk properties, even with the best groundbased and spacebased observatories.

Clearly, if Chiron is the now-active relic it is believed to be, it begs for close up study. Without such investigation, there is no real prospect we will see its surface features, know the true source of its activity, measure its mass and density, or probe the composition of the particulates in its atmosphere. Fortunately, there now appears to be a way to reconnoiter this object, and in doing so, gain a glimpse of what the 10,000 or so QB1s of the Kuiper Disk are really like.

In 1992 and 1993 NASA studied whether missions like a Chiron flyby could be carried out using the investment it is planning to make in the Pluto Fast Flyby (PFF) spacecraft. The answer that came back from this study was yes! Indeed, very few changes would have to be made to the PFF spacecraft design to accomplish a Chiron mission. Chief among the needed changes would be the addition of dust shields to guard against impacts by coma grains, which would pack the hefty punch of a golf ball thrown at 40 miles per hour when struck by the flyby spacecraft passing Chiron at 4 miles per second. The other major change to the spacecraft would be in its instrument payload.

Like the Pluto mission, a Chiron Reconnaissance Flyby would carry a sophisticated CCD camera and infrared mapper. However, because Chiron is easier to reach, additional instruments could be added. Instruments that would likely make the A list for any Chiron mission would be an impact analyzer to study the mass and composition of grains in Chiron's coma, and a mass spectrometer to sniff out the full composition of Chiron's extended atmosphere. It might even be possible to fly a thermal detector to search for places where gas is sublimating from active surface vents. In addition, careful tracking of the spacecraft would accurately measure Chiron's mass. Along with a volume derived from the imaging experiment, such mass measurements would make it possible to determine Chiron's density to see whether the object is more like a giant, fluffy comet or a denser, Pluto/Triton-like ice dwarf.

Mission analysis studies show that the Chiron flyby could reach its target 4.3 years after launch on a giant Titan IV expendable launch vehicle, or 7 years after launch on a much less powerful (and much less expensive), Atlas II launcher. In either case, the trajectory would carry the spacecraft directly from Earth to Chiron, avoiding the need for a complex and radiation-intensive Jupiter flyby. Cost estimates place the mission in the newly-defined *Discovery* class: about $150 million,

plus launcher.

If the lightweight, fast Pluto flyby is carried out, then a follow up Chiron reconnaissance mission would make good use of existing designs, and give humankind its first detailed peek at what seems to be a long-wandering beast from the Sun's icy Kuiper Disk.

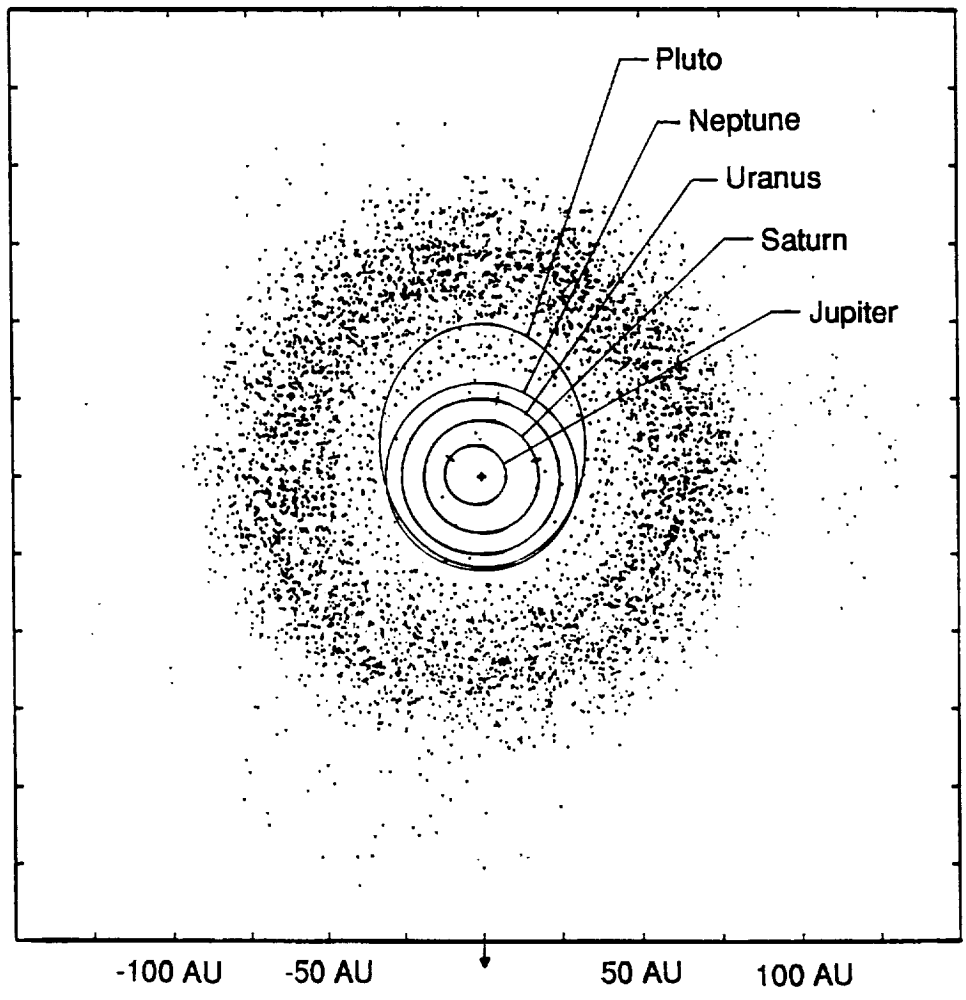
Pluto
Neptune
Uranus
Saturn
Jupiter
-100 AU
-50 AU
50 AU
100 AU

CHIRON'S ORBIT

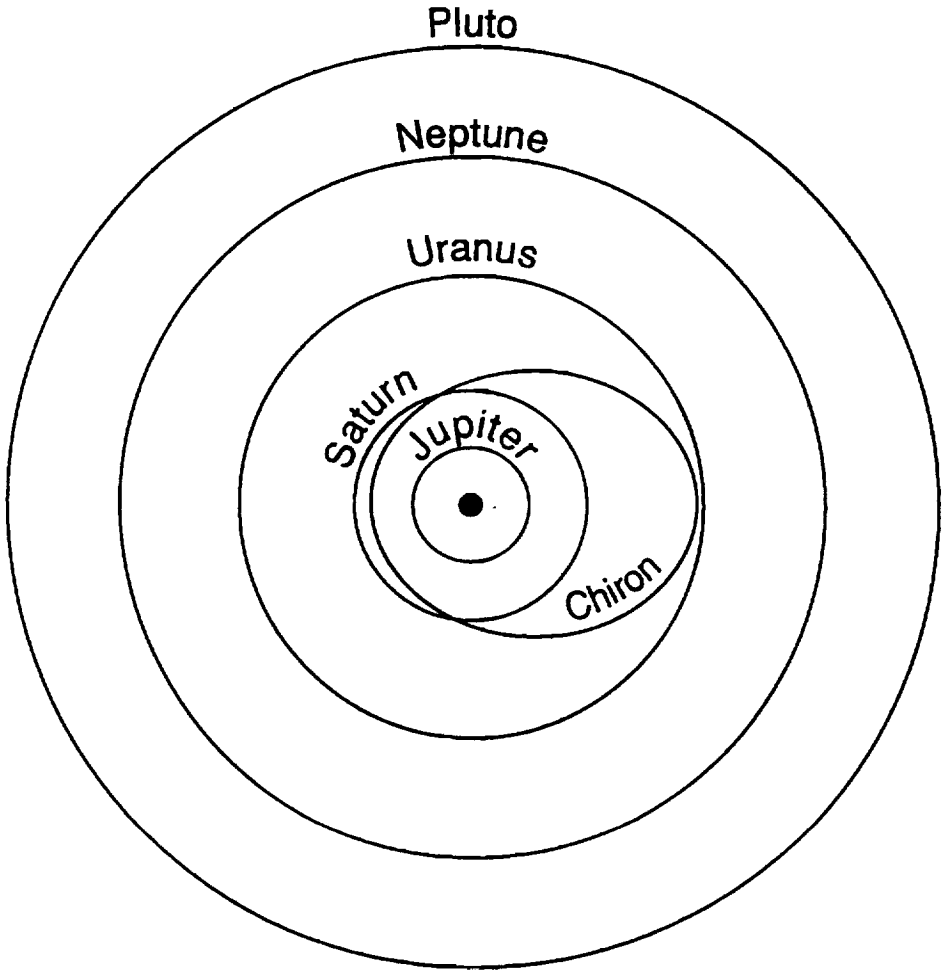

CHIRON SIZE COMPARISON

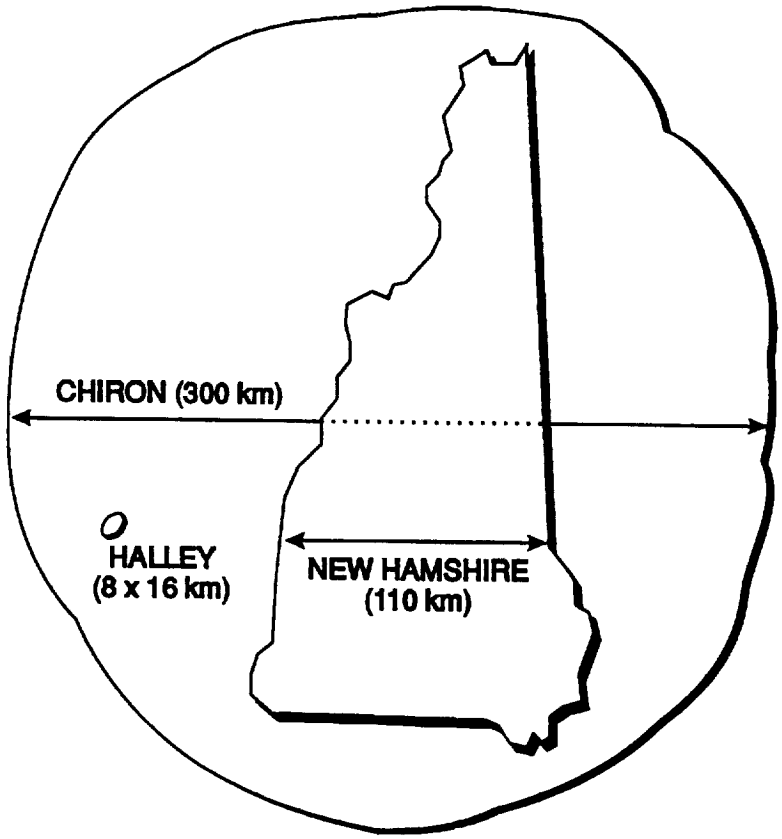

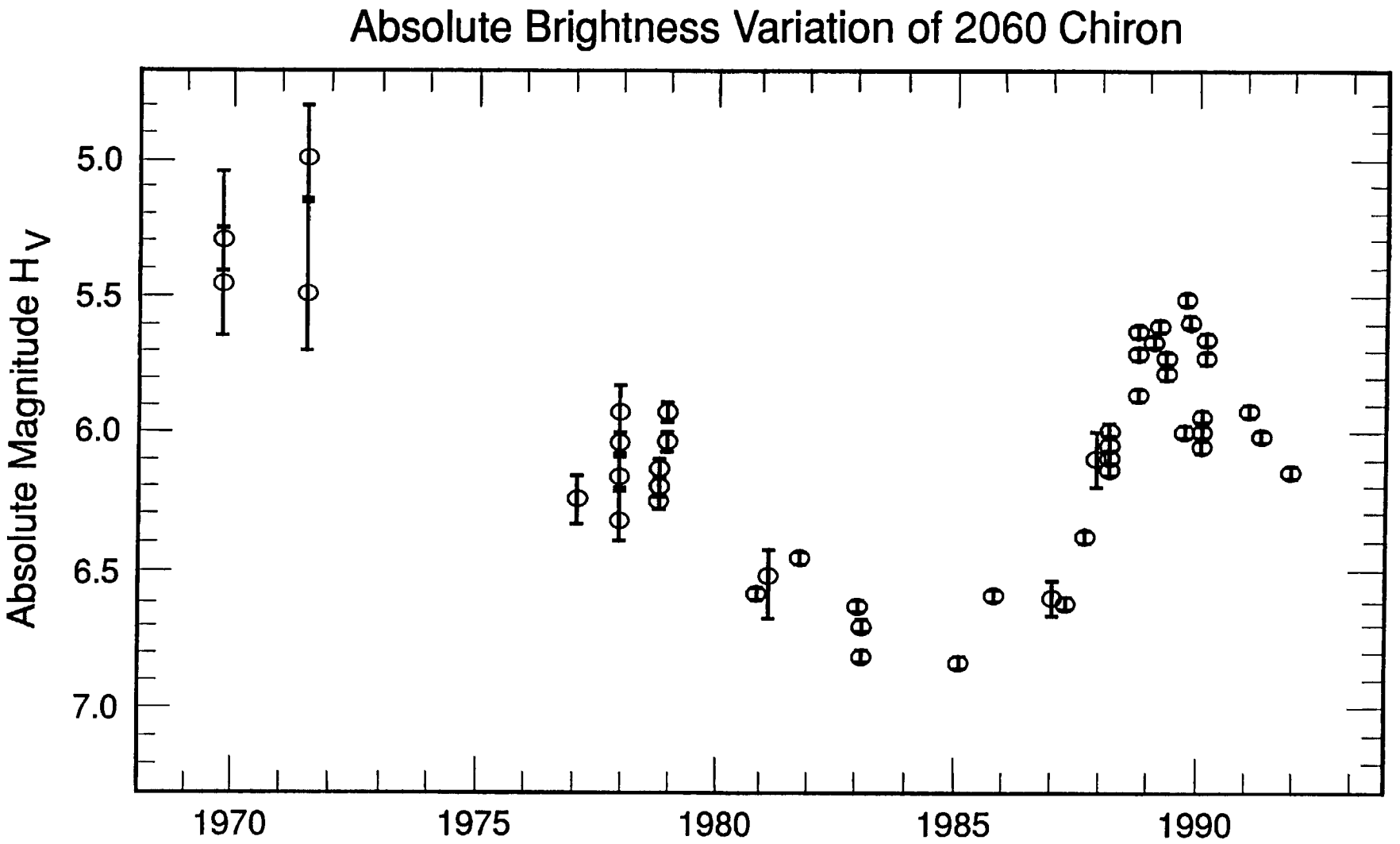
Absolute Brightness Variation of 2060 Chiron
Absolute Magnitude H_V
5.0
5.5
6.0
6.5
7.0
1970
1975
1980
1985
1990

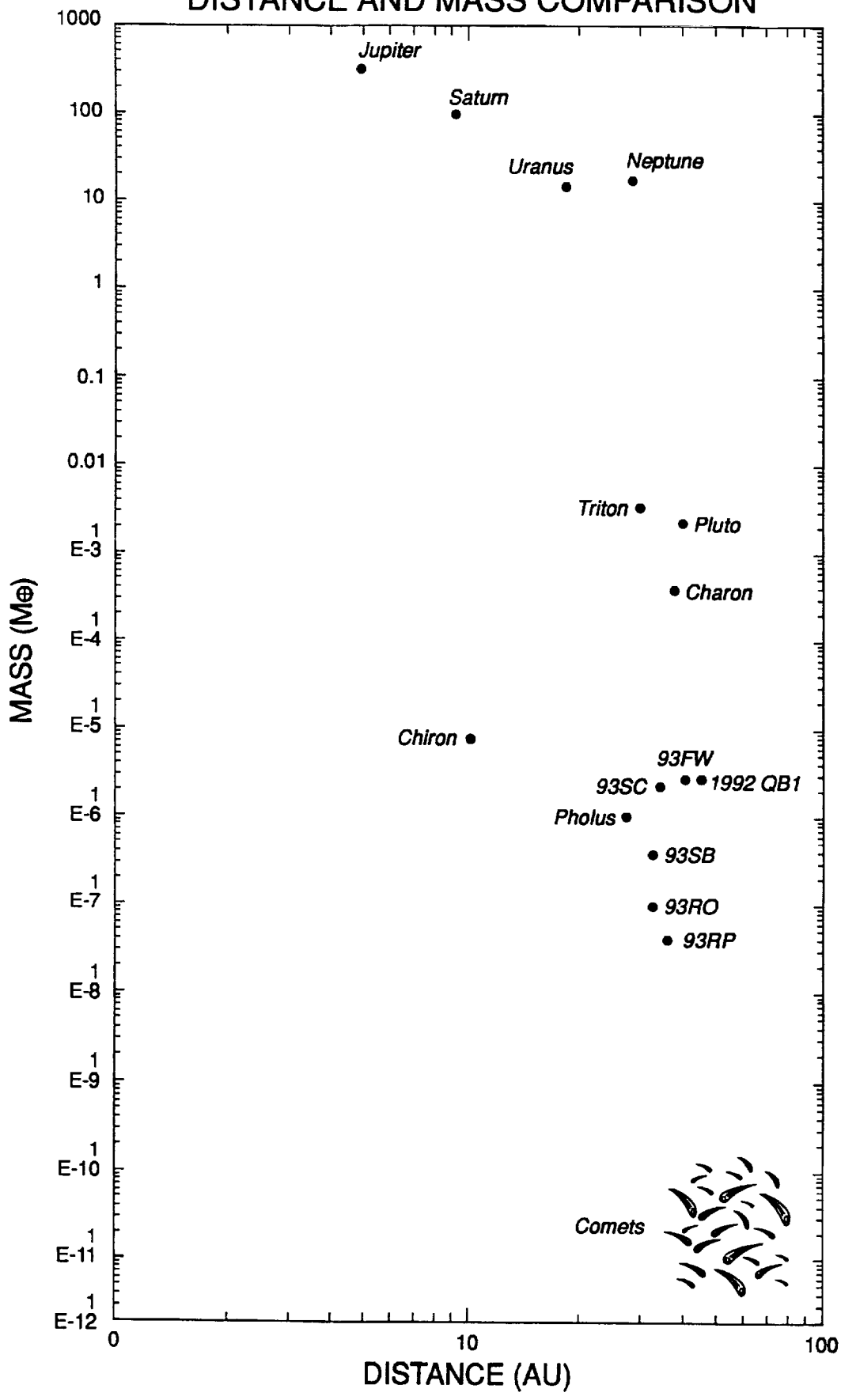
OUTER SOLAR SYSTEM PLANETARY
DISTANCE AND MASS COMPARISON
MASS (M⊕)
1000
100
10
1
0.1
0.01
1 E-3
1 E-4
1 E-5
1 E-6
1 E-7
1 E-8
1 E-9
1 E-10
1 E-11
1 E-12
Jupiter
Saturn
Uranus
Neptune
Triton
Pluto
Charon
Chiron
93FW
93SC
1992 QB1
Pholus
93SB
93RO
93RP
Comets
0
10
100
DISTANCE (AU)

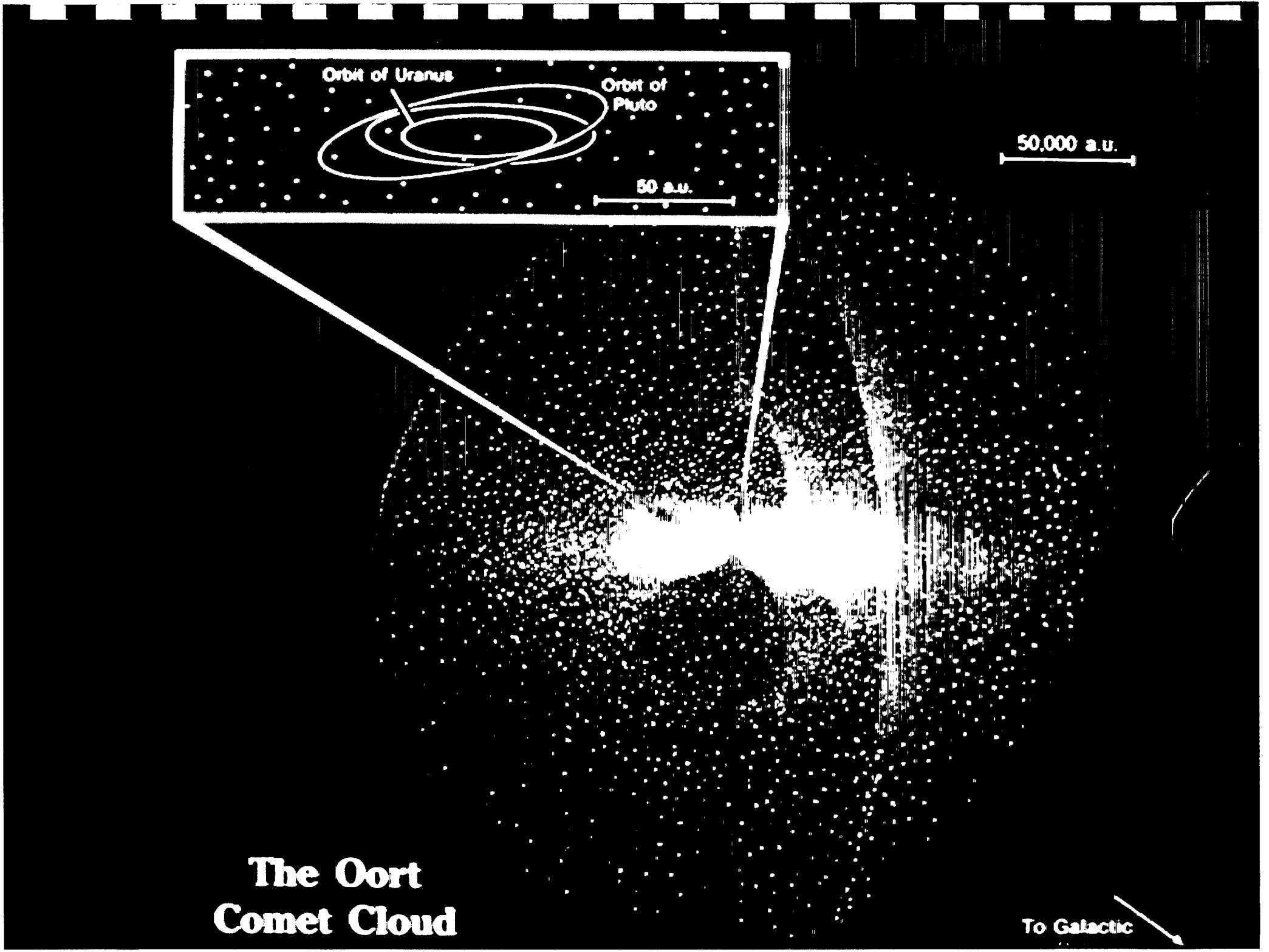
Orbit of Uranus
Orbit of Pluto
50 a.u.
50,000 a.u.
The Oort Comet Cloud
To Galactic